Article

Design and Synthesis of a Novel Series of Orally Bioavailable, CNS-Penetrant, Isoform Selective Phosphoinositide 3-Kinase # Inhibitors (PI3K#) with Potential for the Treatment of Multiple Sclerosis (MS)

Jon H Come, Philip N Collier, James A Henderson, Albert C Pierce, Robert J Davies, Arnaud Le Tiran, Hardwin O'Dowd, Upul K. Bandarage, Jingrong Cao, David Deininger, Ron Grey, Elaine B. Krueger, Derek Bates Lowe, Jianglin Liang, Yusheng Liao, David Messersmith, Suganthi Nanthakumar, Emmanuelle Sizensky, Jian Wang, Jinwang Xu, Elaine Y Chin, Veronique Damagnez, John D. Doran, Wojciech Dworakowski, James P Griffith, Marc D. Jacobs, Suvarna Khare-Pandit, Sudipta Mahajan, Cameron S. Moody, and Alex M. Aronov

J. Med. Chem., **Just Accepted Manuscript** • DOI: 10.1021/acs.jmedchem.8b00085 • Publication Date (Web): 30 May 2018

Design and Synthesis of a Novel Series of Orally Bioavailable, CNS-Penetrant, Isoform Selective Phosphoinositide 3-Kinase γ Inhibitors (PI3Kγ) with Potential for the Treatment of Multiple Sclerosis (MS)

Jon H. Come, Philip N. Collier,* James A. Henderson, Albert C. Pierce, Robert J. Davies, Arnaud Le Tiran, Hardwin O'Dowd, Upul K. Bandarage, Jingrong Cao, David Deininger, Ron Grey, Elaine B. Krueger, Derek B. Lowe, Jianglin Liang, Yusheng Liao, David Messersmith, Suganthi Nanthakumar, Emmanuelle Sizensky, Jian Wang, Jinwang Xu, Elaine Y. Chin, Veronique Damagnez, John D. Doran, Wojciech Dworakowski, James P. Griffith, Marc D. Jacobs, Suvarna Khare-Pandit, Sudipta Mahajan, Cameron S. Moody and Alex M. Aronov**

Vertex Pharmaceuticals Incorporated, 50 Northern Avenue, Boston, Massachusetts 02210, United States

ABSTRACT

The lipid kinase phosphoinositide 3-kinase γ has attracted attention as a potential target to treat a variety of autoimmune disorders, including multiple sclerosis, due to its role in immune

modulation and microglial activation. By minimizing the number of hydrogen bond donors while targeting a previously uncovered selectivity pocket adjacent to the ATP binding site of PI3Kγ, we discovered a series of azaisoindolinones as selective, central nervous system (CNS) penetrant inhibitors of PI3Kγ. This ultimately led to the discovery of **16**, an orally bioavailable compound which showed efficacy in murine experimental autoimmune encephalomyelitis (EAE), a preclinical model of multiple sclerosis.

INTRODUCTION

The phosphoinositide 3-kinases (PI3Ks) are a family of lipid kinases that catalyze the phosphorylation of phosphatidylinositols at the 3-position to generate phosphatidylinositol-3,4,5-triphosphate, which then interacts with effector proteins to impact the regulation of cell growth, differentiation, proliferation, survival, migration, and intracellular trafficking.[1-3] Based on their structure and substrate specificity, the PI3Ks have been divided into three classes. Class I has four members (PI3Kα, PI3Kβ, PI3Kγ, and PI3Kδ) which are heterodimeric complexes that have highly homologous 110 kDa catalytic subunits and bind to a regulatory subunit. Class Ia PI3Ks are activated through tyrosine kinase signaling, while the sole Class Ib member, PI3Kγ, is activated through G-protein-coupled receptor (GPCR) signaling.[1,4,5]

PI3Kα and PI3Kβ are ubiquitously expressed and are important in cell growth, proliferation and survival; deletion of the catalytic subunit of these two isoforms is embryonically lethal in mice.[6-8] Inhibition of PI3Kα/β has mostly been limited to oncology applications.[9-11] In contrast, PI3Kγ and PI3Kδ are mainly expressed in the hematopoietic system,[12] and have been the target of programs in inflammation, autoimmune disease and cardiovascular disease.[13-16] Dual inhibitors of PI3Kγ and PI3Kδ are being investigated for cancer treatment in the clinic.[17-19] Selective inhibition of PI3Kγ may have useful immune-modulating activity, by inhibiting the action of microglia, the brain's resident immune defense against disease and injury. Microglia are activated in response to immunologic stimuli, and are important in maintaining tissue homeostasis and neuronal integrity in the CNS. In neurodegenerative diseases such as MS, microglia may be exposed to non-physiological immune activation. The over-activated microglia contribute to the neurodegeneration by secreting pro-inflammatory mediators such as cytokines, chemokines and reactive oxygen species (ROS).[20,21] The PI3Kγ pathway has been implicated in ROS production and chemokine signaling pathways,[22,23] and progress has been made towards understanding the complex mechanisms involved.[24] Li et al. have shown that systemic treatment with selective PI3Kγ inhibitor AS-604850[23] reduced the number of infiltrated leukocytes in the CNS and alleviated the clinical symptoms of EAE.[25] The same group saw increased myelination and axon number in the spinal chord of EAE mice treated with a PI3Kγ inhibitor.[25] Hence PI3Kγ blockade may be beneficial for the treatment of MS.

Reports of the discovery of selective inhibitors of PI3Kγ are noteworthy given the high sequence homology of the ATP binding sites between PI3K isoforms.[26-33] Designing CNS-penetrant kinase inhibitors is a challenge due to the typical property space characteristic of ATP-competitive kinase inhibitors. Hydrogen-bond donors that interact with kinase hinge elements are a common feature of many kinase pharmacophores.[34] It is also a critical factor in determining the likelihood of CNS penetration.[35] In this report, we describe the design and optimization of a series of isoindolinones as potent, selective, CNS-penetrant inhibitors of PI3Kγ, culminating in the discovery of **16**, an orally bioavailable lead compound showing potential for the treatment of MS.

RESULTS AND DISCUSSION

Previously, we have reported on the discovery of potent and selective benzothiazole urea-based inhibitors of PI3Kγ (Figure 1).[36,37] Selectivity in the benzothiazole series was achieved by accessing a pocket specific to the PI3Kγ isoform. This pocket is made accessible by the movement of Lys883, allowing placement of the distal urea substituent in the newly formed binding cleft. The unique geometry of the urea was key to positioning this substituent. However, the presence of two hydrogen-bond donors in both the benzothiazole[36] and thiazolopiperidine[37] urea-based scaffold classes resulted in low CNS exposure (efflux ratio = 18 for **1** in MDR1-overexpressing MDCK cell line).

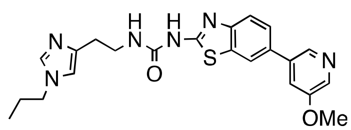

1

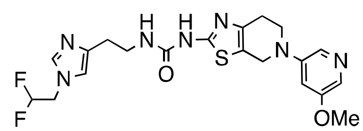

2

Figure 1. Structures of previously reported potent and selective PI3Kγ inhibitors.

In pursuit of our goal of discovering CNS-penetrant, isoform selective inhibitors of PI3Kγ, the urea-based scaffolds were evolved in accordance to the following criteria: (1) maintain access to the selectivity pocket; (2) keep no more than a single hydrogen bond acceptor to the hinge region; (3) remove all formal hydrogen bond donors. Of all the designs that were explored, the isoindolinone scaffold design proved the most compelling. We hypothesized that the isoindolinone carbonyl group would provide a hydrogen bond acceptor to the backbone NH of hinge residue Val882, while the N2-substituent would allow access to the previously described selectivity pocket (Figure 2). An aromatic proton would be positioned in place of the urea NH donor. While it was uncertain how significant the CH••O pseudo hydrogen bond would be, we felt confident based on literature precedent, that it would be tolerated, and that its introduction would lead to compounds with lower affinity for PgP-mediated efflux pumps.[38,39] Finally, the C5 substituent on the isoindolinone scaffold would provide potency, guided by SAR knowledge gained from our earlier work.

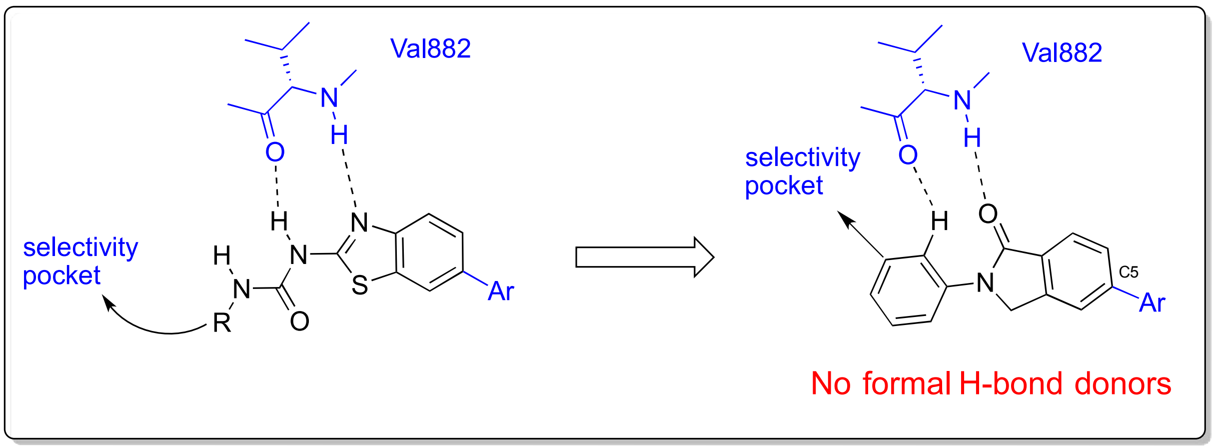

Figure 2. Rational design of the isoindolinone scaffold shows key design features: (a) contacts between inhibitor and hinge region Val882; (b) vector toward selectivity pocket; (c) C5 vector to aromatic substituent.

We designed and synthesized an initial library of 80 compounds with variation at the isoindolinone C5 position and at the meta-position of the phenyl ring attached to N2. We biased the C5 set towards substituents that were shown to possess higher affinity in the benzothiazole series,[36] and focused work on meta-substituted phenyls at N2, as we felt this position afforded the best vector to reach the selectivity pocket.

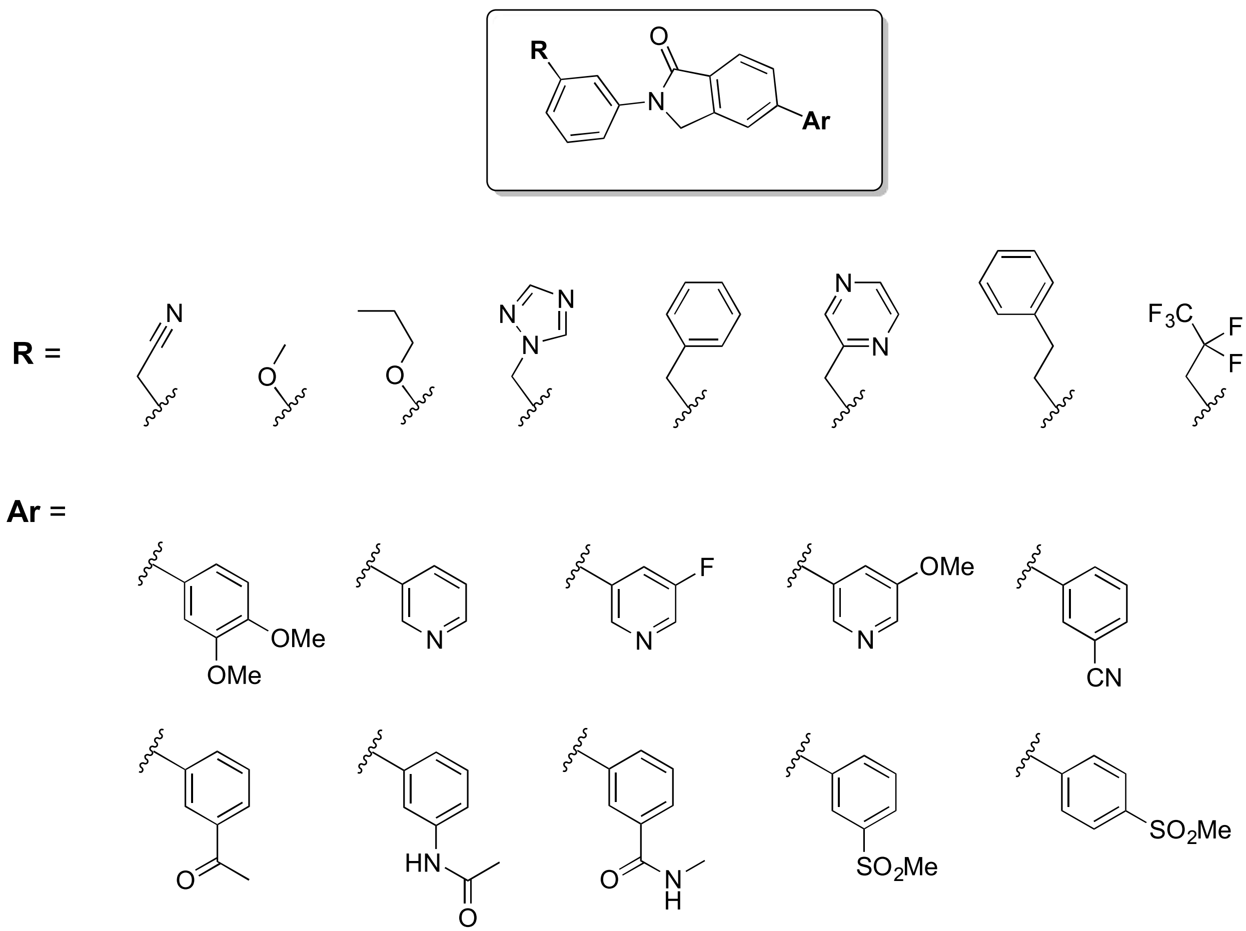

Figure 3. Library design for initial exploration of the isoindolinone scaffold

From the initial set, two hits were identified, including **3** (Table 1), which inhibited PI3Kγ with a Ki of 160 nM and was greater than 20-fold selective against PI3Kα and PI3Kβ, and 7-fold selective against PI3Kδ. Encouraged by these results, we sought to improve the potency and metabolic stability of the series, while capitalizing on prior SAR knowledge at C5.[36, 37] Consistent with previous results from the benzothiazole series, conversion of the C5 substituent from 3,4-dimethoxyphenyl to 3,4-dimethoxy-5-pyridinyl increased PI3Kγ affinity fourfold (Table 1, **4**) while maintaining isoform selectivity. PK studies revealed that compound **4** had high plasma clearance in rats (see Table 1) so we attempted to improve the metabolic stability by reducing compound lipohilicity. Replacing the N2 (cyanomethyl)phenyl moiety with an N-

(cyanomethyl)pyrazole substituent (Table 1, **5**) led to higher PI3Kγ affinity and reduced clearance in rats, while selectivity against other Class 1 PI3Ks was largely maintained. Finally, introduction of a nitrogen atom in place of C4 in the isoindolinone core further increased PI3Kγ affinity and lowered in vitro and in vivo clearance (Table 1, **6**). The reduced intrinsic clearance and Rat IV clearance observed on transitioning from **3** to **6** correlated with a corresponding drop in lipophilicity (logD @ pH 7.4: 4.1 for **3**, 1.7 for **6**).

Table 1. Initial Optimization of Isoindolinone Library hit **3**.

Structure	Cpd	PI3Kγ[a] Ki	Fold Selectivity over:			Hepatocyte int. Cl[b] Rat/Human	Rat IV Cl[c]
			PI3Kα	PI3Kβ	PI3Kδ		
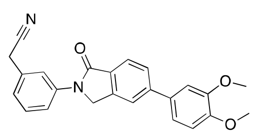	**3**	0.16	>25	>25	7	111/26	116
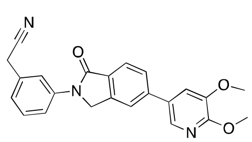	**4**	0.035	40	11	16	88/30	160
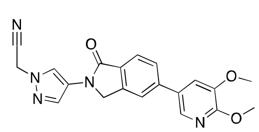	**5**	0.006	51	27	17	ND	56
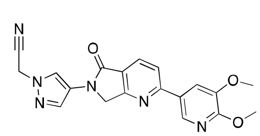	**6**	0.004	40	25	12	7.9/10	27

[a]All enzyme data are expressed in μM. [b]CL expressed in μL/min/million cells. [c]CL expressed in mL/min/Kg.

The X-ray crystal structure of **6** in complex with PI3Kγ confirmed that it bound in a manner envisioned in our design, with the carbonyl of the azaisoindolinone acting as a hinge binding motif, while the nitrile substituent pointed towards the selectivity pocket (Figure 4). The proton at the 5-position of the pyrazole is directed at the carbonyl of Val882, forming the aromatic CH••O hydrogen bond as designed and mimicking the urea NH donor interaction observed in the benzothiazole series (Figure 5). PI3Kγ affinity is enhanced by the dimethoxypyridine group which makes (a) key water-mediated hydrogen bonds between the pyridine nitrogen atom and Tyr867 and Asp841, residues which are conserved across PI3K isoforms, and (b) favorable protein contacts with Lys833, similar to those seen in the benzothiazole series.[36] An overlay of **6** with one of our more selective benzothiazole ureas is shown in Figure 5. **6** does not occupy the selectivity pocket in PI3Kγ to the same extent seen in the case of ureas such as **1** and does not induce a movement of the Lys883 sidechain as seen in the benzothiazole urea scaffold, suggesting that azaisoindolinones such as **6**, derive PI3Kγ selectivity in a somewhat different manner.

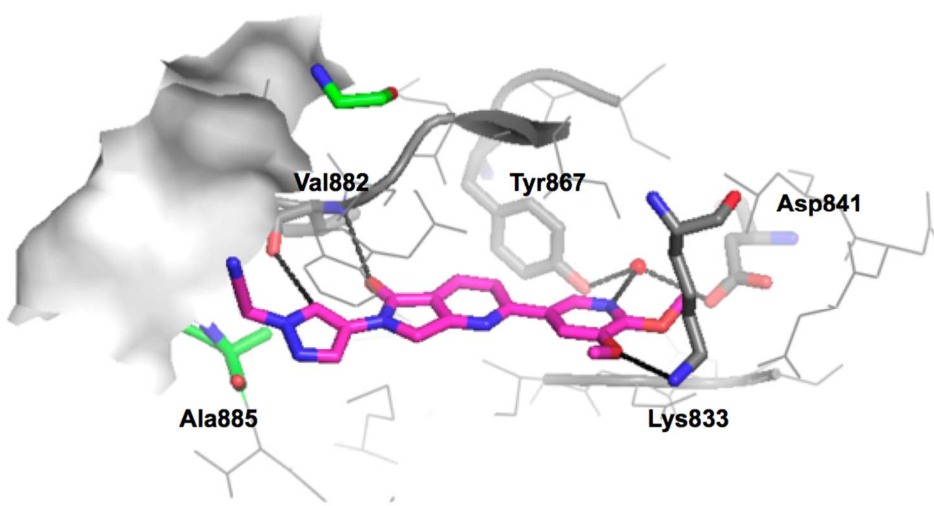

Figure 4. X-ray structure of azaisoindolinone **6** bound to PI3Kγ (PDB code 6C1S). The ligand makes a bidentate hinge binding interaction with Val882. The dimethoxypyridine group

enhances affinity by making three favorable interactions to the ATP binding site (Lys833, and water mediated interactions with Tyr867 and Asp841). Ala885, which drove a degree of isoform selectivity in the benzothiazole series, is highlighted.

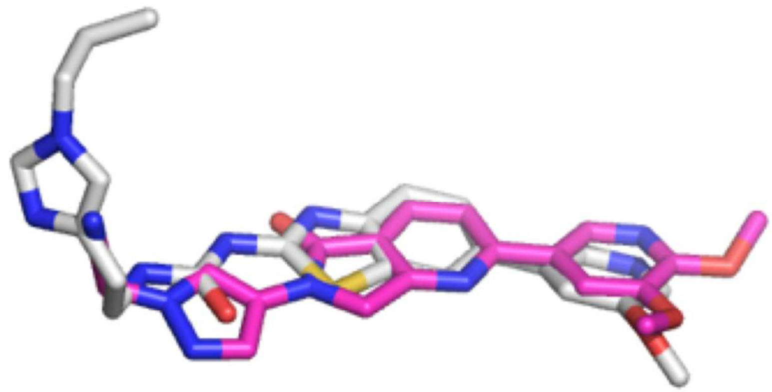

Figure 5. Overlay of azaisoindolinone **6** and benzothiazole urea **1** as they bind to PI3Kγ. The lactam carbonyl oxygen atom fulfills the role of the nitrogen atom in the benzothiazole by making a hydrogen bond to the backbone NH of Val882. The pyrazole aromatic C-H donor mimics the role of the urea H-bond donor of the benzothiazole scaffold.

Compound **6** had an acceptable rat PK profile with a clearance of 27 mL/min/kg. However, upon further investigation, it was established that dealkylation of the pyrazole to produce compound **7** was a major route of metabolism, potentially generating cyanide via oxidation of the methylene of the cyanomethyl substituent (see Supporting Information for details). Consequently, we surveyed a number of alternative substituents to replace the pyrazole cyanomethyl group, and the results of this study are shown in Table 2.

Des-alkyl compound **7** displayed good selectivity against class Ia PI3Ks but was a substrate for P-glycoprotein efflux protein (efflux ratio = 9 in MDR1-MDCK), disfavoring entry into the CNS. Isoform selectivity was generally improved on transitioning from methyl to larger alkyl groups. This may be due to PI3K isoform residue differences at Ala885 as described in our previous work.[36] In the other PI3K class Ia isoforms, this residue is a serine which, we hypothesize, may negatively interact with larger lipophilic pyrazole *N*-alkyl groups. The lower PI3Kγ affinity observed for **13** is potentially due to steric disruption of the hinge binding pyrazole CH••O hydrogen bond. By replacing the cyanomethyl with a trifluoroethyl group (compound **10**), it was possible to maintain potency and selectivity while eliminating the potential for cyanide generation. P-gp mediated efflux was reduced in pyrazole *N*-alkyl compounds **8 – 13**, generally correlating with the lower PSA of these compounds relative to **6**.

Table 2. Pyrazole *N*-alkyl group SAR

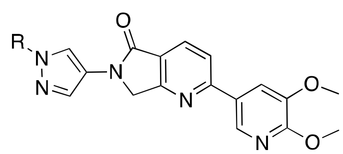

R	Cpd	PI3Kγ Ki μM	Fold Selectivity			PSA Å^2	MDCK-MDR1 ER
			PI3Kα	PI3Kβ	PI3Kδ		
CH_2CN	**6**	0.003	50	31	16	106	4.7
H	**7**	0.011	34	32	42	93	8.7
Me	**8**	0.06	5	9	3	82	2.5
Et	**9**	0.008	25	39	14	82	2.2
CH_2CF_3	**10**	0.004	65	31	13	82	0.8
CH_2CCH	**11**	0.009	11	25	12	82	2.3
CH_2CHF_2	**12**	0.009	22	12	5	82	2.6
$C(Me)_2CN$	**13**	0.028	15	25	10	106	2.1
CH_2CH_2CN	**14**	0.02	11	10	4	106	ND

We also evaluated substitutions at C3, which allowed us to explore interesting vectors out of the plane of the rest of the molecule. While addition of a (*R*)-methyl group at C3 (Table 3, **16**) maintained a biochemical profile similar to before, we observed an improvement in rat IV clearance from 56 to 20 mL/min/kg and half life from 1.1 to 3.3 h. Substitution of C3 with a gem-dimethyl group lowered clearance still further to 6.3 mL/min/kg, but activity and selectivity were somewhat eroded.

Advanced lead compounds **10** and **15-17**, were tested in various assays to determine their potency in inhibiting PI3Kγ-dependent signaling and function. Chemokines such as MCP-1 bind to their receptors, resulting in activation of the PI3Kγ signaling pathway. MCP-1 activation leads to PI3Kγ-mediated Akt phosphorylation, and P-Akt following MCP-1 introduction was used as a marker of PI3Kγ activity. Compounds **10**, **15-17** were found to inhibit MCP-1 induced Akt phosphorylation in THP-1 cells. Furthermore, compound **16** was found to inhibit MCP-1 induced Akt phosphorylation in splenocytes with an IC_{50} of 0.21 μM (+/-0.15; n=3). PI3Kγ functional activity was measured in TNF-α primed human neutrophils and monocytes via the generation of ROS. Compound **16** showed reduction in ROS production after stimulation with *N*-formyl-Met-Leu-Phe (fMLP), with an IC_{50} of 0.14 μM (0.50 μM in whole blood), giving us greater confidence in our mechanistic hypothesis, and the potential of our selective PI3Kγ inhibitors in the treatment of multiple sclerosis.

No cross activity was shown for **16** against a diverse panel of serine/threonine and tyrosine kinases and against a wider panel of kinases (50/50 < 15% inhibition at 10 μM, see Supporting Information). Additionally, **16** showed excellent selectivity against a diverse set of 75 non-kinase targets (all < 25% inhibition at 10 μM). The only substantial cross activity of **16** was against the PI3K-related serine/threonine kinase DNA-PK (K_i = 0.26 μM).

Table 3. Azaisoindolinone C3 SAR

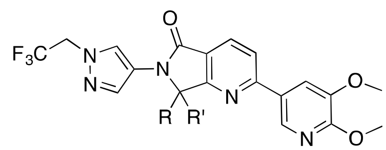

R, R'	Cpd	PI3Kγ Ki µM	Fold Selectivity			THP-1[a,b] (MCP-1) IC_{50}	Rat Hep int. Cl[c]	Rat IV PK[d] Cl, $T_{1/2}$
			PI3Kα	PI3Kβ	PI3Kδ			
H, H	**10**	0.004	65	31	13	0.28	ND	56, 1.1
(*S*)-Me, H	**15**	0.007	28	18	7	0.21	9.2	15, 4.7
(*R*)-Me, H	**16**	0.004	60	10	14	0.17	7.0	20, 3.3
Me, Me	**17**	0.011	33	12	10	0.34	ND	6.3, 6.6

[a]Cell data are expressed in µM; [b]the procedure involves monitoring the phosphorylation state of Ser-473; [c]Cl expressed in µL/min/million cells; [d]Cl expressed in mL/min/Kg and $T_{1/2}$ in h

Additional profiling of compound **16** is shown in Tables 4 and 5. The compound showed good cross species IV PK profiles, presenting low to moderate clearance values and adequate half lives. Based on in-vitro data and allometric scaling from preclinical species, the predicted human whole blood clearance, volume of distribution and half-life were 3.3 mL/min/Kg, 4.2 L/Kg and 15 h, respectively. The predicted human oral bioavailability was 66%. Compound **16** was highly permeable and showed no efflux in Caco-2 or MDR1-MDCK assays, thereby indicating potential for good penetration at the blood-brain barrier. When taken together, these data suggested that exposure of **16** in the CNS would be sufficient to modulate PI3Kγ in an *in vivo* model. Compound **16** was also assessed for its ability to cause drug-drug interactions, and showed no inhibition against a panel of recombinant human CYP isoforms, and no potential for time-dependent inhibition of CYPs. Finally, compound **16** showed no cardiovascular liabilities (hERG IC_{50} of > 30 µM) or genotoxicity (negative in AMES assay).

Table 4. Cross species comparison of PK parameters and hepatocyte intrinsic clearance of **16**

	Cl[a]	$T_{1/2}$ (h)	V_{ss}[b]	%F	Hepatocyte Intrinsic Cl[c]
Rat	8.8	2.8	32	70	5
Dog	19	3.2	5.2	28	12
Monkey	4.0	2.4	0.8	39	7
Human	-	-	-	-	4

[a]Units of mL/min/Kg; [b]units of L/Kg; [c]units of μL/min/M cells

Table 5. Further profiling of compound **16**

MW, logD (pH 7.4), PSA	433, 3.0, 82
Rat PO PK @ 3 mg/Kg (%F, $T_{1/2}$, AUC, Cmax)	100, 5.1 h, 7.2,[a] 0.7[b]
MDR1-MDCK B-A/A-B; A-B	0.7, 50[c]
Caco-2 B-A/A-B; A-B	0.9, 24[c]
CYP inhibition 3A4, 2C9, 2D6	all >30 μM
P450, TDI	No issues
5-Strain Ames	No issues
hERG (manual patch) IC_{50}	>30 μM

[a]Units of μg*h/mL; [b]Units of μg/mL; [c]Units of x10^{-6} cm/s.

On the basis of its overall favorable profile, and given that it had met our design criteria, compound **16** was selected as the preferred compound for *in vivo* pharmacological evaluation. **16** was evaluated in murine EAE, a well-established model of multiple sclerosis. It has previously been shown that treatment with PI3Kγ inhibitor AS-604850, ameliorated the clinical symptoms of EAE mice.[25] PI3Kγ deletion in knockout mice has also mitigated the clinical symptoms of EAE compared to PI3Kγ$^{+/+}$ controls.[25] In our study, C57BL6 mice were immunized by injection of myelin oligodendrocyte glycoprotein (MOG) in complete Freund's adjuvant containing Mycobacterium tuberculosis (see Supporting Information for full details). Following injection of pertussis toxin, animals were evaluated for disease symptoms. On reaching a clinical score of 0.5-1, animals were dosed with vehicle, **16** or positive control fingolimod (FTY-720). At doses of 3, 10 and 30 mg/Kg BID of **16**, we observed significant reduction in clinical disability scores as shown in Figure 6, with efficacy comparable to FTY-720. Based on the aforementioned Caco-2/MDR1-MDCK data, we expected compound **16** to display good brain penetration. Gratifyingly, we found unbound brain exposure at 4 h post dose was comparable (3 mg/kg) or exceeded (10 and 30 mg/kg) IC_{50} (ROS functional assay), indicating ample target coverage at the selected doses (Table 6). These results give us greater confidence in PI3Kγ inhibition as an approach for the potential treatment of MS.

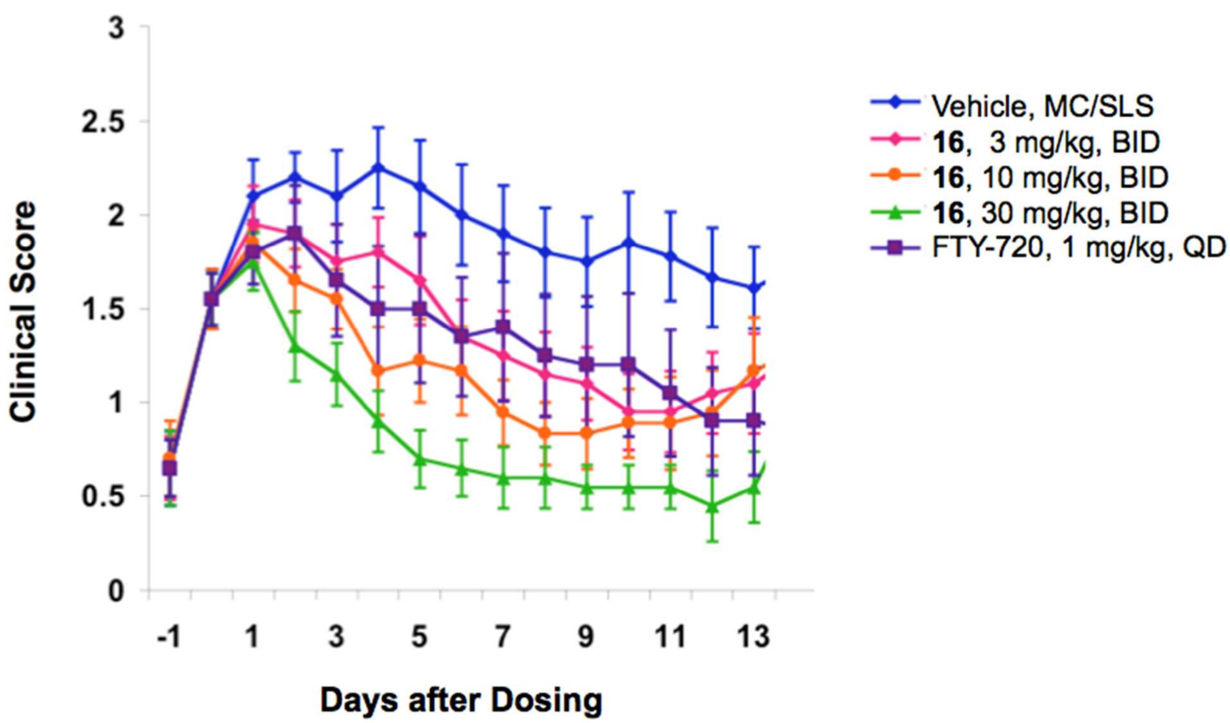

Figure 6. Treatment with **16** attenuates clinical symptoms of EAE mice. Animals were dosed orally BID with **16**, or QD with FTY-720 on reaching a clinical score of 0.5-1. Plot indicates clinical EAE scores as a function of time after EAE onset.

Table 6. Unbound brain concentrations of **16** from EAE study[a]

Time (h)	**Concentration** (nM)		
	3 mg/kg	10 mg/Kg	30 mg/Kg
4	398 (±89)	1017 (±230)	1594 (±303)
14	87 (±45)	294 (±128)	764 (±96)

[a]Brain samples collected 4 and 14 h after the last dose in the EAE study (see Supporting Information). Unbound concentrations calculated with brain homogenate; fraction unbound values (*fu 16%*) obtained from *in vitro* equilibrium dialysis experiments.

Chemistry. The synthesis of 5-arylisoindolinones **3 - 5** are depicted in Schemes 1 and 2. The isoindolinone ring was formed by an alkylation/ring closure one-pot sequence. Subsequent Suzuki-Miyaura coupling provided **3** and **4**. The 4-azaisoindolinone core of compounds **6**, **7**, **10-14** was prepared in an overall similar manner to above, albeit using radical halogenation to provide intermediates **24** and **25** (Schemes 3 and 4). Ortho-chlorination of intermediate **25** was achieved by treatment of its pyridine *N*-oxide **26** with phosphorus oxychloride.

The pyrazole *N*-alkyl substituent at position 2 of the azaisoindolinine ring was varied in a late stage alkylation step on pyrazole **7**, yielding compounds **10-12** and **14** (Scheme 4). The cyano(dimethyl)methyl group of compound **13** was introduced by alkylation of 4-nitro-1*H*-pyrazole with 2-bromo-2-methyl-propanamide (Scheme 5). Compounds **8** and **9** were synthesized from fully elaborated 1-alkyl-4-aminoprazoles using the one-pot alkylation/ring closure as the key step (Scheme 6). Substituents were introduced at the azaisoindolinone C3 position by a deprotonation/alkylation sequence (Scheme 7) and preparatory chiral HPLC was used to separate enantiomers **15** and **16**.

Scheme 1. Synthesis of isoindolinones **3** and **4**[a]

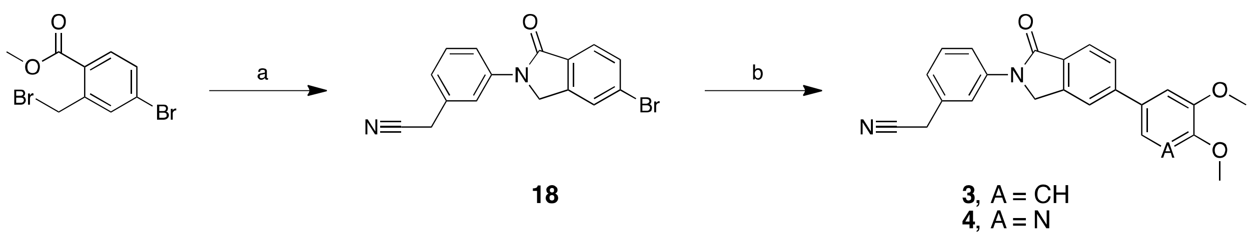

[a]Reagents and conditions: (a) 2-(3-aminophenyl)acetonitrile, DMF, 110 ºC; (b) (3,4-dimethoxyphenyl)boronic acid (for **3**) or 2,3-dimethoxy-5-(4,4,5,5-tetramethyl-1,3,2-dioxaborolan-2-yl)pyridine (for **4**), Pd(dppf)Cl_2, Cs_2CO_3, DMSO, H_2O, 100 ºC.

Scheme 2. Synthesis of isoindolinone **5**[a]

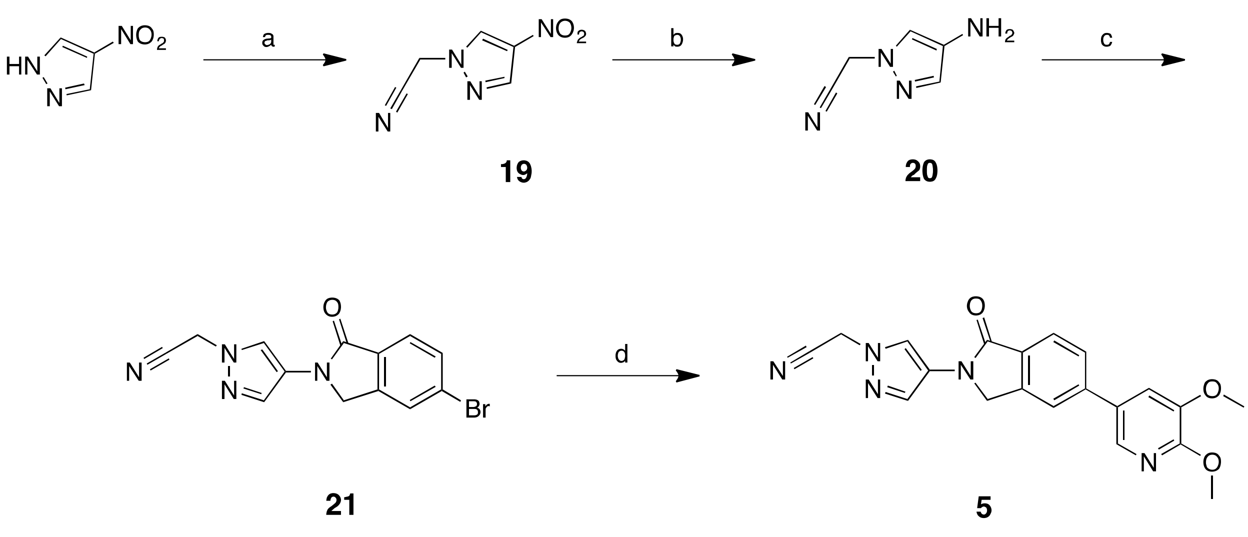

[a]Reagents and conditions: (a) iodoacetonitrile, Cs_2CO_3, DMF; (b) Fe, NH_4Cl, EtOH, 75 ºC; (c) methyl 4-bromo-2-(bromomethyl)benzoate, DMF, 100 ºC; (d) 2,3-dimethoxy-5-(4,4,5,5-tetramethyl-1,3,2-dioxaborolan-2-yl)pyridine, Pd(dppf)Cl_2, Cs_2CO_3, DMSO, H_2O, 100 ºC.

Scheme 3. Synthesis of isoindolinone **6**[a]

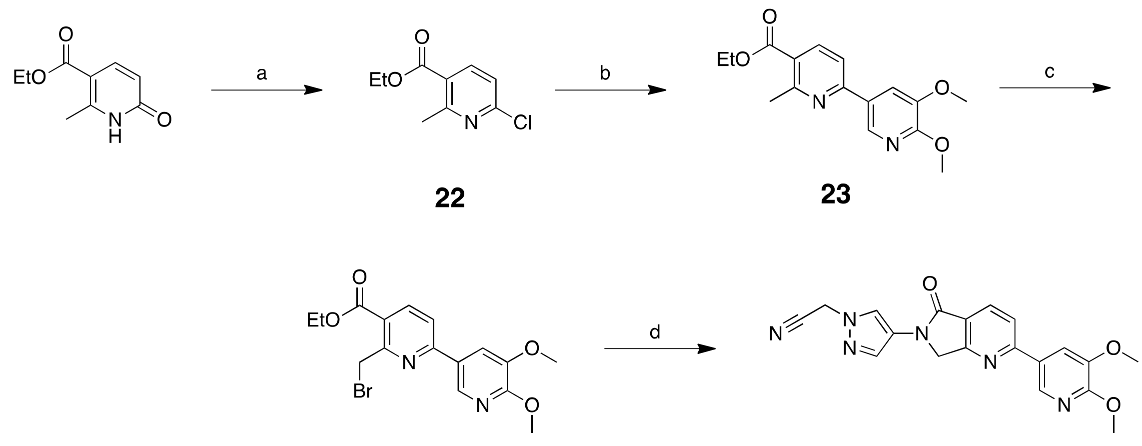

22 **23** **24** **6**

[a]Reagents and conditions: (a) $POCl_3$, 100 ºC; (b) 2,3-dimethoxy-5-(4,4,5,5-tetramethyl-1,3,2-dioxaborolan-2-yl)pyridine, $Pd(PPh_3)_4$, Na_2CO_3, $MeCN/H_2O$ (3/1), 90 ºC; (c) NBS, AIBN, K_2CO_3, CCl_4, 80 ºC; (d) 2-(4-amino-1*H*-pyrazol-1-yl)acetonitrile, Na_2CO_3, DMF, 90 ºC.

Scheme 4. Synthesis of azaisoindolinones **7**, **10-12**, **14**[a]

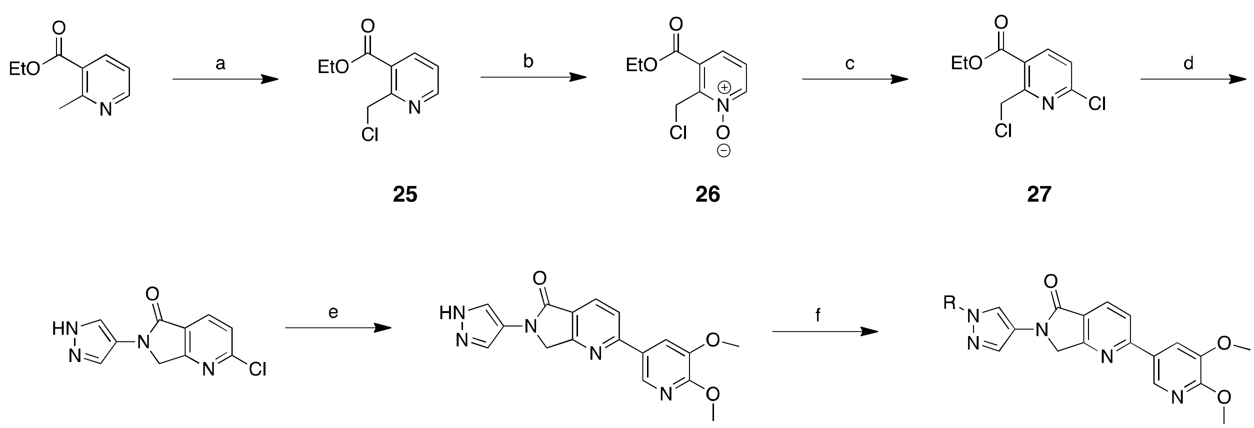

25 **26** **27** **28** **7**

10, R = CH_2CF_3
11, R = CH_2CCH
12, R = CH_2CHF_2
14, R = CH_2CH_2CN

[a]Reagents and conditions: (a) 1,3,5-trichloro-1,3,5-triazinane-2,4,6-trione, DCM; (b) *m*-CPBA, DCM; (c) $POCl_3$; (d) 1*H*-pyrazol-4-amine, DIPEA, DMF, 80 ºC; (e) 2,3-dimethoxy-5-(4,4,5,5-tetramethyl-1,3,2-dioxaborolan-2-yl)pyridine, $Pd(PPh_3)_4$, Na_2CO_3, DMF, 90 ºC; (f) 2,2,2-trifluoroethyl trifluoromethanesulfonate (for **10**), 3-chloroprop-1-yne (for **11**), 2-bromo-1,1-difluoro-ethane (for **12**), 3-bromopropanenitrile (for **14**), Cs_2CO_3, DMF, microwave or conventional heating.

Scheme 5. Synthesis of azaisoindolinone **13**[a]

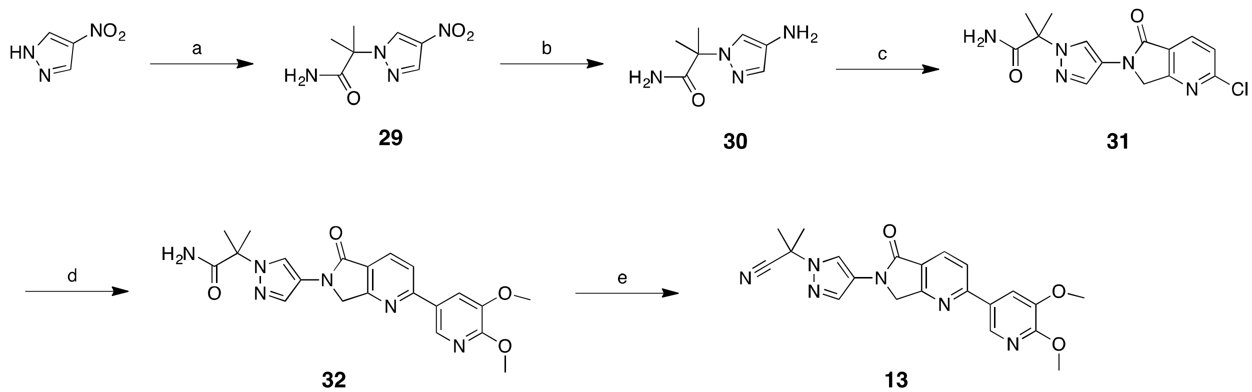

[a]Reagents and conditions: (a) 2-bromo-2-methyl-propanamide, K_2CO_3, DMF; (b) H_2 (40 psi), Pd/C (10%), MeOH; (c) ethyl 6-chloro-2-(chloromethyl)pyridine-3-carboxylate, DIPEA, IPA, 80 ºC; (d) 2,3-dimethoxy-5-(4,4,5,5-tetramethyl-1,3,2-dioxaborolan-2-yl)pyridine, $Pd(PPh_3)_4$, Na_2CO_3, DMF, 80 ºC; (e) Burgess reagent, DCM/MeCN (1:1).

Scheme 6. Synthesis of alkylpyrazoles **8** and **9**[a]

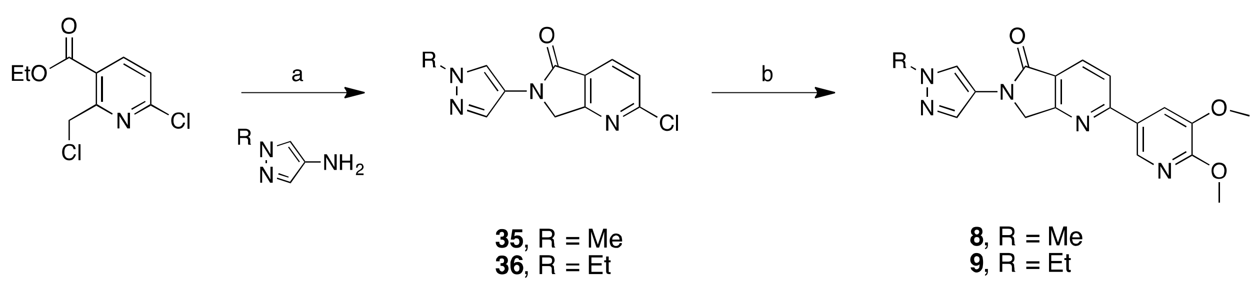

[a]Reagents and conditions: (a) DIPEA, iPrOH (for **35**) or MeCN (for **36**), reflux; (b) 2,3-dimethoxy-5-(4,4,5,5-tetramethyl-1,3,2-dioxaborolan-2-yl)pyridine, $Pd(PPh_3)_4$, K_2CO_3, dioxane, microwave, 150 ºC.

Scheme 7. Synthesis of 7-substituted-azaisoindolinones **15 - 17**[a]

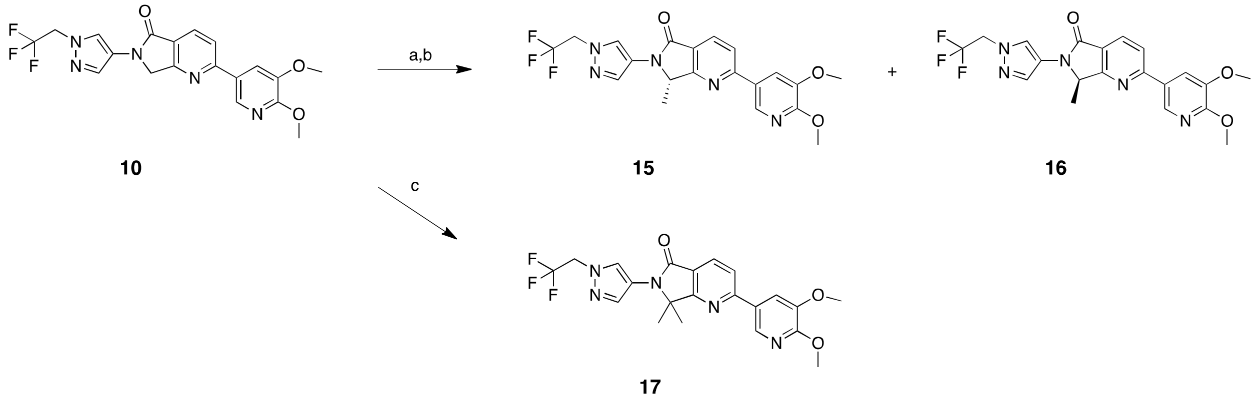

[a]Reagents and conditions: (a) NaH, MeI, THF; (b) chiral HPLC separation; (c) NaH, MeI, DMF.

CONCLUSION

We have designed and synthesized a series of high affinity, isoform selective, CNS-penetrant and orally bioavailable inhibitors of PI3Kγ. Guided by structural data from our earlier reported work in this area, our scaffold design strategy was biased towards hinge-binding motifs lacking formal H-bond donor atoms. This yielded compounds without the efflux liabilities associated with our earlier scaffolds. Further optimization culminated in the discovery of **16**, which demonstrated efficacy in murine EAE, providing support for the further evaluation of this mechanism for the treatment of multiple sclerosis.

EXPERIMENTAL SECTION

Chemistry. All commercially available reagents and anhydrous solvents were used without further purification. An inert atmosphere of nitrogen was used for reactions involving air of moisture sensitive reagents. Purity assessment for final compounds based on analytical HPLC: column, 4.6 x 50 mm Waters YMC Pro-C18 column, 5 μM, 120Å. Mobile phases are as follows: A, water with 0.2% formic acid; B, acetonitrile with 0.2% formic acid; gradient, 10-90% B in 3 min with 5 min run time. The flow rate is 1.5 mL/min. All final compounds were ≥ 95% purity. Mass samples were analyzed on a Waters/MicroMass ZQ, ZMD, Quattro LC, or Quatro II mass spectrometer operated in a single MS mode with electrospray ionization. Samples were introduced into the mass spectrometer using flow injection (FIA) or chromatography. The mobile phase for all mass analysis consisted of acetonitrile-water mixtures with either 0.2% formic acid or ammonium formate. High-resolution mass measurements were performed on a Thermo QExactive mass spectrometer with a heated electrospray source operated in positive ion mode. ^{1}H NMR spectra were recorded either using a Bruker Avance 400 (400 MHz) or a Bruker Avance II-300 (300 MHz) instrument at ambient temperature and are quoted in ppm relative to a tetramethylsilane internal standard, or by referencing on the chemical shift of the deuterated solvent. Data are displayed in following format: chemical shift, multiplicity (s = singlet, d = doublet, t = triplet, q = quartet, br = broad, m = multiplet), coupling constants, and number of protons. The column chromatography was performed using Teledyne ISCO RediSep Normal Phase (35-70 microns) or RediSep Gold Normal Phase (25-40 microns) silica flash columns using a Teledyne ISCO Combiflash Companion or Combiflash Rf purification system. Preparative reversed phase chromatography was carried out using a Gilson 215 liquid handler coupled to a UV_vis 156 Gilson detector, an Agilent Zorbax SB-C18 column, 21.2 x 100 mm, a linear gradient from 10-90% acetonitrile in water over 10 min (0.1% TFA); the flow rate was 20 mL/min. Microwave-assisted reactions were performed using a CEM Discover S-Class microwave instrument (single mode microwave reactor) with 48-position autosampler. Temperature was monitored during microwave reactions by a vertically sensored infrared temperature sensor, which comes as a standard feature of the CEM Discover S-Class system.

2-(3-(5-(3,4-Dimethoxyphenyl)-1-oxoisoindolin-2-yl)phenyl)acetonitrile (**3**). Step 1: A 10 mL microwave vial was charged with 2-(3-aminophenyl)acetonitrile (500 mg, 3.78 mmol), methyl 4-bromo-2-(bromomethyl)benzoate (1.2 g, 3.8 mmol) and DMF (3 mL). The vial was sealed and microwaved at 110 °C for 25 min. The reaction mixture was diluted with MeOH (50 mL) and an off-white solid filtered off and dried under vacuum to give **18** (703 mg, 57%) as a white solid. ^{1}H NMR (300 MHz, DMSO-d_6) δ 7.96 (d, J = 7.3 Hz, 2H), 7.83 - 7.71 (m, 3H), 7.47 (t, J = 8.0 Hz, 1H), 7.18 (d, J = 7.6 Hz, 1H), 5.03 (s, 2H), 4.10 (s, 2H). Mass spectrum (ESI) *m/z* 328.3 $[M + H]^+$.

Step 2: A microwave vial was charged with **18** (100 mg, 0.31 mmol), (3,4-dimethoxyphenyl)boronic acid (60 mg, 0.34 mmol), Cs_2CO_3 (200 mg, 0.61 mmol), DMSO (2 mL) and H_2O (0.3 mL). The solution was sparged with nitrogen for 10 min and Pd(dppf)Cl_2 (12 mg, 0.015 mmol) was added. The vial was sealed and microwaved at 100 °C for 10 min. The reaction mixture was poured into EtOAc/H_2O and the organic layer passed through a plug of florisil and concentrated to a residue which was triturated with MeOH, filtered and dried under vacuum to give **3** (80 mg, 68%) as a white solid. ^{1}H NMR (300 MHz, DMSO-d_6) δ 8.03 (s, 1H), 7.95 (s, 1H), 7.86 - 7.81 (m, 3H), 7.48 (t, J = 8.0 Hz, 1H), 7.34 - 7.31 (m, 2H), 7.17 (d, J = 7.6 Hz, 1H), 7.10 (d, J = 9.0 Hz, 1H), 5.07 (s, 2H), 4.11 (s, 2H), 3.88 (s, 3H), 3.82 (s, 3H). HRMS found for $M^+ + 1$, 385.1547, $C_{24}H_{20}N_2O_3$ requires 385.1546.

2-(3-(5-(5,6-Dimethoxypyridin-3-yl)-1-oxoisoindolin-2-yl)phenyl)acetonitrile (**4**). A 10 mL microwave vial was charged with **18** (50 mg, 0.15 mmol), 2,3-dimethoxy-5-(4,4,5,5-tetramethyl-1,3,2-dioxaborolan-2-yl)pyridine (44 mg, 0.17 mmol), Cs_2CO_3 (100 mg, 0.31 mmol), DMSO (1 mL) and H_2O (150 μL). The solution was sparged with nitrogen for 10 min and Pd (dppf)Cl_2 (6 mg, 0.008 mmol) was added. The vial was sealed and microwaved at 100 °C for 10 min. The reaction mixture was poured into EtOAc/H_2O and the organic layer was passed through a plug of florisil and concentrated to a residue which was triturated with MeOH, filtered and dried under vacuum to give **4** (59 mg, 69%) as a white solid. ^{1}H NMR (300 MHz, DMSO-d_6) δ 8.12 (d, J = 1.9 Hz, 1H), 8.02 (d, J = 8.2 Hz, 2H), 7.88 (m, 3H), 7.65 (d, J = 1.9 Hz, 1H), 7.49 (t, J = 8.0 Hz, 1H), 7.18 (d, J = 7.7 Hz, 1H), 5.09 (s, 2H), 4.11 (s, 2H), 3.94 (s, 3H), 3.92 (s, 3H). HRMS found for $M^+ + 1$, 386.1501, $C_{23}H_{29}N_3O_3$ requires 386.1499.

2-(4-(5-(5,6-Dimethoxypyridin-3-yl)-1-oxoisoindolin-2-yl)-1H-pyrazol-1-yl)acetonitrile (**5**). Step 1: To a flask containing 4-nitro-1H-pyrazole (1.0 g, 8.84 mmol) and Cs_2CO_3 (2.88 g, 8.84 mmol) in DMF (30 mL) was added iodoacetonitrile (1.48 g, 8.84 mmol). After stirring at room temperature for 30 min, the reaction mixture was poured into H_2O/EtOAc and the organic layer was dried and concentrated to give **19** (1.1 g, 86%) as an oil. ^{1}H NMR (300 MHz, $CDCl_3$) δ 8.38 (s, 1H), 8.17 (s, 1H), 5.16 (s, 2H).

Step 2: A 5L 3-neck-flask equipped with a mechanical stirrer was charged with **19** (50 g, 0.32 mol), ethanol (1 L), NH_4Cl (106 g, 1.97 mol) and water (250 mL). Iron (73.4 g, 1.3 mol) was added to this solution and the reaction was sparged with nitrogen and heated to 75 °C internal temp (took 30 min to reach this temp). After 3 h at 75 °C, the reaction mixture was filtered through Celite, washed with ethanol (3 x 500 mL) and the filtrate was evaporated to dryness on the rotovap. DCM (1 L) was added followed by sodium sulfate and the resulting suspension was filtered. The collected solids were washed with DCM (3 x 400 mL). The filtrate was concentrated to dryness to give **20** as a tan solid (22.8 g, 57%). ^{1}H NMR (300 MHz, $CDCl_3$) δ 7.24 (s, 1H), 7.13 (s, 1H), 4.97 (s, 2H), 3.02 (br s, 2H). Mass spectrum (ESI) *m/z* 122.9 $[M + H]^+$.

Step 3: In a 10 mL microwave tube, **20** (200 mg, 1.6 mmol) and methyl 4-bromo-2-(bromomethyl)benzoate (250 mg, 0.81 mmol) were combined in DMF (2 mL) and heated to 110 °C for 20 min. The reaction mixture was poured into EtOAc/H_2O and the organic layer was separated, dried and concentrated to provide an oil which was triturated with MeOH. The precipitated solid was filtered off to give **21** (65 mg, 13%). ^{1}H NMR (300 MHz, DMSO-d_6) δ 8.35 (s, 1H), 7.91 (d, J = 2.2 Hz, 2H), 7.71 (q, J = 8.1 Hz, 2H), 5.53 (s, 2H), 4.88 (s, 2H). Mass spectrum (ESI) *m/z* 316.9 $[M + H]^+$.

Step 4: **21** (65 mg, 0.2 mmol) was combined with 2,3-dimethoxy-5-(4,4,5,5-tetramethyl-1,3,2-dioxaborolan-2-yl)pyridine (54 mg, 0.2 mmol), and Cs_2CO_3 (133 mg, 0.41 mmol), DMSO (2 mL) and H_2O (0.2 mL), Pd(dppf)Cl_2 (14.6 mg, 0.02 mmol) in a 10 mL microwave tube and microwaved at 100 °C for 10 min. The reaction mixture was poured in to EtOAc/H_2O and the organic layer passed through a plug of florisil washing with EtOAc. The filtrate was concentrated to a residue which was triturated with MeOH and filtered to give **5** (32 mg, 40%) as a white solid. ^{1}H NMR (300 MHz, DMSO-d_6) δ 8.37 (s, 1H), 8.11 (d, J = 2.0 Hz, 1H), 7.97 (m, 2H), 7.84 (m, 2H), 7.64 (d, J = 2.0 Hz, 1H), 5.55 (s, 2H), 4.93 (s, 2H), 3.93 (s, 3H), 3.91 (s, 3H). HRMS found for $M^+ + 1$, 376.1407, $C_{20}H_{17}N_5O_3$ requires 376.1404.

2-(4-(2-(5,6-Dimethoxypyridin-3-yl)-5-oxo-5,7-dihydro-6H-pyrrolo[3,4-b]pyridin-6-yl)-1H-pyrazol-1-yl)acetonitrile (**6**). Step 1: A mixture of ethyl 2-methyl-6-oxo-1,6-

dihydropyridine-3-carboxylate (5.92 g, 32.6 mmol) in phosphorous oxychloride (45 mL) was heated at 90 °C for 1 h. After cooling, the reaction mixture was concentrated under reduced pressure and ice water was added to the residue, followed by addition of 28% ammonium hydroxide to adjust the pH to 7. The resulting white solid was collected by filtration, washed with ice water, and dried under high vacuum to give **22** (6.18 g, 95%). ^{1}H NMR (300 MHz, $CDCl_3$) δ 8.18 (d, J = 8.2 Hz, 1H), 7.27 (d, J = 8.2 Hz, 1H), 4.40 (q, J = 7.1 Hz, 2H), 2.84 (s, 3H), 1.42 (t, J = 7.4, 3H). Mass spectrum (ESI) m/z 200.2 $[M + H]^+$.

Step 2: A mixture of **22** (4.0 g, 20.0 mmol), 2,3-dimethoxy-5-(4,4,5,5-tetramethyl-1,3,2-dioxaborolan-2-yl)pyridine (5.84 g, 22.0 mmol), $Pd(PPh_3)_4$ (1.15 g, 1.00 mmol), and sodium carbonate (6.37 g, 60.1 mmol) in a mixture of acetonitrile/water (3:1, 90 mL) was heated at 90 °C under an atmosphere of nitrogen for 4 h. After cooling, the volatiles were removed under reduced pressure and the residue dissolved in DCM. After washing with water, the organic phase was dried (Na_2SO_4), filtered, and concentrated under reduced pressure. The residue was purified by silica gel chromatography (0-20% EtOAc/hexanes) to give **23** (5.8 g, 96% yield). ^{1}H NMR (300 MHz, $CDCl_3$) δ 8.27 (d, J = 1.8 Hz, 1H), 8.17 (d, J = 8.2 Hz, 1H), 7.83 (d, J = 1.8 Hz, 1H), 7.52 (d, J = 8.3 Hz, 1H), 4.32 (q, J = 7.1 Hz, 2H), 4.01 (s, 2H), 3.93 (s, 3H), 2.83 (s, 3H), 1.34 (t, J = 7.1 Hz, 3H). ESMS m/z 303.41 (M^+ + 1).

Step 3: To a solution of **23** (4.4 g, 14.6 mmol) in CCl_4 (75 mL) was added AIBN (239 mg, 1.46 mmol) and NBS (1.7 g, 9.55 mmol). The mixture was stirred at 80 °C for 1.5 h under an atmosphere of nitrogen. The reaction mixture was filtered and concentrated. The residue was purified by silica gel chromatography (20% EtOAc/hexanes) to give a mixture of starting material and **24** (4.44 g, 47%, ca. 60% pure). ^{1}H NMR (300 MHz, $CDCl_3$) δ 8.39 (d, J = 2.0 Hz, 1H), 8.35 (d, J = 8.3 Hz, 1H), 7.95 (d, J = 2.0 Hz, 1H), 7.74 (d, J = 8.3 Hz, 1H), 5.12 (s, 2H), 4.47 (q, J = 7.1 Hz, 2H), 4.11 (s, 3H), 4.03 (s, 3H), 1.47 (t, J = 7.1 Hz, 3H). Mass spectrum (ESI) m/z 303.4 $[M + H]^+$.

Step 4: A solution of ethyl 6-(bromomethyl)-5',6'-dimethoxy-[2,3'-bipyridine]-5-carboxylate **24** (2.2 g, 3.46 mmol) in DMF (40 mL) at 0 °C was added dropwise over 2 h to a suspension of 2-(4-amino-1*H*-pyrazol-1-yl)acetonitrile (844 mg, 6.9 mmol) and sodium carbonate (732 mg, 6.9 mmol) in DMF (20 mL). After addition was complete, the reaction mixture was stirred at 0 °C for 2 h and heated at 80 °C for 15 h. Additional sodium carbonate (732 mg) was added and the reaction mixture was heated at 90 °C for an additional 7 h. After cooling, the mixture was poured into water and a precipitate formed. The solid was collected by filtration, washed with methyl t-butyl ether, and dried under high vacuum to provide **6** (450 mg, 32%). ^{1}H NMR (300 MHz, DMSO-d_6) δ 8.56 (d, J = 1.9 Hz, 1H), 8.39 (s, 1H), 8.22 (d, J = 8.2 Hz, 1H), 8.20 – 8.03 (m, 1H), 8.03 (s, 1H), 7.97 (s, 1H), 5.56 (s, 2H), 5.00 (s, 2H), 3.96 (s, 3H), 3.92 (s, 3H). HRMS found for $M^+ + 1$, 377.1359, $C_{19}H_{16}N_6O_3$ requires 377.1356.

2-(5,6-Dimethoxypyridin-3-yl)-6-(1*H*-pyrazol-4-yl)-6,7-dihydro-5*H*-pyrrolo[3,4-*b*]pyridin-5-onec (7). Step 1: A round bottom flask was charged with ethyl 2-methylpyridine-3-carboxylate (50 g, 303 mmol), 1,3,5-trichloro-1,3,5-triazinane-2,4,6-trione (106 g, 454 mmol) and DCM (250 mL). The solution was stirred for at room temperature for 12 h and then diluted with saturated Na_2CO_3 (600 mL) and DCM (600 mL). The organic layer was separated, washed with saturated Na_2CO_3 followed by brine, then dried over Na_2SO_4, filtered and concentrated to provide **25** (59.8 g, 99%) as a pale yellow oil. ^{1}H NMR (300 MHz, $CDCl_3$) δ 8.64 (dd, J = 4.8, 1.7 Hz, 1H), 8.21 (dd, J = 7.9, 1.7 Hz, 1H), 7.28 (dd, J = 7.9, 4.8 Hz, 1H), 5.04 (s, 2H), 4.36 (q, J = 7.1 Hz, 2H), 1.34 (q, J = 7.4 Hz, 3H). Mass spectrum (ESI) m/z 200.0 $[M + H]^+$.

Step 2: To a round bottom flask containing **25** (25.5 g, 128 mmol) in DCM (250 mL) was added mCPBA (32.4 g, 141 mmol). The reaction was stirred at room temperature for 12 h. The reaction mixture was then washed with saturated aqueous Na_2CO_3, brine, and then dried over Na_2SO_4, filtered and concentrated. The crude material was purified through a silica plug (300 g) while eluting with EtOAc. Product containing fractions were concentrated to yield **26** (20.8 g, 75%). ^{1}H NMR (300 MHz, MeOH-d$_4$) δ 8.68 (dd, J = 4.9, 1.7 Hz, 1H), 8.36 (dd, J = 7.9, 1.7 Hz, 1H), 7.51 (dd, J = 7.9, 4.9 Hz, 1H), 5.10 (s, 2H), 4.43 (q, J = 7.1 Hz, 2H), 1.43 (t, J = 7.1 Hz, 3H). Mass spectrum (ESI) *m/z* 216.7 $[M + H]^+$.

Step 3: **26** (14.7 g, 68.3 mmol) was dissolved in $POCl_3$ (209 g, 1.37 mol) and heated to 90 °C for 36 h under N_2. The reaction was concentrated to dryness, diluted with DCM (300 mL) and washed with water. The organics were dried over sodium sulfate, filtered, and concentrated to dryness. The crude residue was purified by flash chromatography (25%-50% EtOAc/hexanes) to provide **27** (9.4 g, 59%). ^{1}H NMR (300 MHz, $CDCl_3$) δ 8.26 (d, J = 8.3 Hz, 1H), 7.40 (d, J = 8.3 Hz, 1H), 5.08 (s, 2H), 4.45 (q, J = 7.1 Hz, 2H), 1.51 – 1.36 (m, 3H). Mass spectrum (ESI) *m/z* 234.3 $[M + H]^+$.

Step 4: To a round bottom flask containing 1H-pyrazol-4-amine (2.04 g, 24.6 mmol) in DMF (23 mL) at room temperature was added DIEA (3.75 g, 5 mL, 29.0 mmol), followed by dropwise addition of a solution of **27** (4.53 g, 19.4 mmol) in DMF (23 mL) over 10 min. The reaction was stirred for 2 h at RT and then heated to 80 °C for 12 h. To this solution was added MeOH (100 mL) and the reaction was allowed to cool. The solid precipitate was filtered and washed with MeOH (2 x 25 mL). The solid was dried under high vacuum for 8 h to yield **28** (3.02 g, 66%). ^{1}H NMR (300 MHz, DMSO-d_6) δ 12.91 (s, 1H), 8.17 (d, J = 8.1 Hz, 1H), 8.12 (s, 1H), 7.90 (d, J = 1.8 Hz, 1H), 7.66 (d, J = 8.1 Hz, 1H), 4.92 (s, 2H). Mass spectrum (ESI) *m/z* 235.0 $[M + H]^+$.

2-(5,6-Dimethoxypyridin-3-yl)-6-(1-methyl-1H-pyrazol-4-yl)-6,7-dihydro-5H-pyrrolo[3,4-b]pyridin-5-one (**8**). *Step 1:* 1-Methylpyrazol-4-amine (46 mg, 0.479 mmol), ethyl 6-chloro-2-(chloromethyl)pyridine-3-carboxylate (112 mg, 0.479 mmol), and DIPEA (110 mL, 0.655 mmol) were combined in isopropanol (4 mL). The reaction was heated to 100 °C under N_2 for 12 h, concentrated to dryness, then MeOH (5 mL) was added and the slurry was filtered and dried under vacuum to provide **35** (90 mg, 77%). Mass spectrum (ESI) *m/z* 249.2 $[M + H]^+$.

Step 2: A 10 mL microwave vial was charged with **35** (71 mg, 0.285 mmol), 2,3-dimethoxy-5-(4,4,5,5-tetramethyl-1,3,2-dioxaborolan-2-yl)pyridine (91 mg, 0.343 mmol), K_2CO_3 (2M, 2 mmol) and dioxane (2 mL). The solution was sparged with nitrogen for 5 min, followed by addition of $Pd(PPh_3)_4$ (16.4 mg, 0.0142 mmol). The reaction was sealed and microwaved at 150 °C for 10 min. After cooling, the reaction was diluted with EtOAc and the organics were separated and concentrated. To the crude residue was added MeOH (10 mL), and the resulting precipitate was collected by filtration, washed with MeOH (2 x 10 mL) and dried under vacuum to provide **8** (42 mg, 42%). ^1H NMR (300 MHz, $CDCl_3$) δ 8.40 (d, J = 2.0 Hz, 1H), 8.24 – 8.14 (m, 2H), 7.88 (dd, J = 13.9, 5.0 Hz, 2H), 7.65 (s, 1H), 4.85 (s, 2H), 4.12 (s, 3H), 4.04 (s, 3H), 3.98 (d, J = 4.1 Hz, 3H). HRMS found for $M^+ + 1$, 352.1407, $C_{18}H_{17}N_5O_3$ requires 352.1404.

2-(5,6-Dimethoxypyridin-3-yl)-6-(1-ethyl-1H-pyrazol-4-yl)-6,7-dihydro-5H-pyrrolo[3,4-b]pyridin-5-one (**9**). Step 1: 1-Ethylpyrazol-4-amine (1.06 g, 9.49 mmol), ethyl 6-chloro-2-(chloromethyl)pyridine-3-carboxylate (2.00 g, 8.54 mmol), and DIPEA (1.66 g, 2.2 mL, 12.8 mmol) were combined in acetonitrile (21 mL). The reaction was stirred at rt for 5 min, then heated to 80 °C under N_2 for 18 h. MeOH was added and the reaction slurry was filtered, dried under vacuum to give **36** (1.08 g, 48%) as a light grey solid. ^1H NMR (300 MHz, DMSO-d_6) δ

8.19 (d, J = 7.8 Hz, 2H), 7.80 (s, 1H), 7.67 (d, J = 8.1 Hz, 1H), 4.91 (s, 2H), 4.17 (q, J = 7.3 Hz, 2H), 1.38 (t, J = 7.3 Hz, 3H). Mass spectrum (ESI) m/z 263.2 $[M + H]^+$.

Step 2: A 10 mL microwave vial was charged with **36** (75 mg, 0.285 mmol), 2,3-dimethoxy-5-(4,4,5,5-tetramethyl-1,3,2-dioxaborolan-2-yl)pyridine (91 mg, 0.343 mmol), K_2CO_3 (2M, 1 mL) and dioxane (2 mL). The solution was sparged with nitrogen for 5 min, followed by addition of $Pd(PPh_3)_4$ (16.4 mg, 0.0142 mmol). The reaction was sealed and microwaved at 150 °C for 10 min. After cooling, the reaction was diluted with EtOAc (1 mL) and the organics were separated and concentrated. To the crude residue was added MeOH (10 mL), and the resulting precipitate was collected by filtration, washed with MeOH (2 x 10 mL) and dried under vacuum to provide **9** (40 mg, 38%). ^1H NMR (300 MHz, $CDCl_3$) δ 8.40 (d, J = 2.0 Hz, 1H), 8.27 – 8.15 (m, 2H), 7.88 (dd, J = 14.6, 5.0 Hz, 2H), 7.66 (d, J = 0.5 Hz, 1H), 4.86 (s, 2H), 4.25 (q, J = 7.3 Hz, 2H), 4.13 (s, 3H), 4.04 (s, 3H), 1.56 (t, J = 7.3 Hz, 3H). HRMS found for M^+ + 1, 366.1561, $C_{19}H_{19}N_5O_3$ requires 366.1560.

2-(5,6-Dimethoxy-3-pyridyl)-6-[1-(2,2,2-trifluoroethyl)pyrazol-4-yl]-7H-pyrrolo[3,4-b]pyridin-5-one (**10**) Step 1: A 250 mL round bottom flask fitted with a reflux condenser was charged with **28** (1.0 g, 4.26 mmol), sodium carbonate (1 M, 8.52 mmol), 2,3-dimethoxy-5-(4,4,5,5-tetramethyl-1,3,2-dioxaborolan-2-yl)pyridine (1.35 g, 5.11 mmol) and DMF (85 mL). The solution was sparged with nitrogen for 30 min, and then $Pd(PPh_3)_4$ (985 mg, 0.852 mmol) was added. The reaction was heated to 90 °C under a nitrogen atmosphere. After 18 h, the reaction mixture was then diluted with MeOH (100 mL), cooled and the resulting solid was collected by vacuum filtration. The solid was washed with additional MeOH (2 x 50 mL) and dried under high vacuum to yield **7** (1.30 g, 90%) as pale green solid. ^1H NMR (300 MHz, DMSO-d_6) δ 12.82 (br s, 1H), 8.55 (d, J = 1.9 Hz, 1H), 8.18 (s, 2H), 8.09 – 7.96 (m, 3H), 4.98 (s, 2H), 4.01 – 3.85 (m, 6H). HRMS found for $M^+ + 1$, 338.1249, $C_{17}H_{15}N_5O_3$ requires 338.1247.

Step 2: A 10 mL microwave vial was charged sequentially with **7** (50 mg, 0.137 mmol), cesium carbonate (89 mg, 0.275 mmol), DMF (1 mL), and 2,2,2-trifluoroethyl trifluoromethanesulfonate (64 mg, 0.275 mmol). The vial was sealed and microwaved at 120 °C for 5 min. The reaction was diluted with 10 mL of water and extracted with EtOAc (30 mL). The organics were concentrated and purified by reverse phase chromatography (C18 column, 5-100% MeCN/H_2O containing 0.1% TFA) The product containing fractions were diluted with DCM, washed with saturated sodium bicarbonate and passed through a phase separator. The organics were concentrated to yield **10** (7.1 mg, 12%). ^{1}H NMR (300 MHz, DMSO-d_6) δ 8.56 (d, J = 1.9 Hz, 1H), 8.40 (s, 1H), 8.21 (t, J = 6.1 Hz, 2H), 7.99 (d, J = 1.9 Hz, 1H), 7.95 (s, 1H), 5.21 (d, J = 9.1 Hz, 2H), 5.01 (s, 2H), 3.96 (s, 3H), 3.92 (s, 3H). HRMS found for $M^+ + 1$, 420.1280, $C_{19}H_{16}F_3N_5O_3$ requires 420.1278.

2-(5,6-Dimethoxypyridin-3-yl)-6-(1-(prop-2-yn-1-yl)-1H-pyrazol-4-yl)-6,7-dihydro-5H-pyrrolo[3,4-b]pyridin-5-one (**11**). A 10 mL microwave vial was charged with **7** (70 mg, 0.208 mmol), cesium carbonate (135 mg, 0.415 mmol), DMF (700 µL) and 3-chloroprop-1-yne (77 mg, 75 µL, 1.04 mmol). The vial was sealed and microwaved at 120 °C for 15 min. The reaction was worked-up by trituration with water (2 mL) and subsequent filtration. The solid was washed with water (2 x 10 mL), filtered, and dried under vacuum to provide **11** (57.3 mg, 70%) as a brown powder. ^{1}H NMR (300 MHz, DMSO-d_6) δ 8.55 (d, J = 1.9 Hz, 1H), 8.29 (s, 1H), 8.24 – 8.13 (m, 2H), 7.97 (t, J = 5.3 Hz, 1H), 7.86 (s, 1H), 5.09 (d, J = 2.5 Hz, 2H), 4.98 (s, 2H), 3.95 (s, 3H), 3.93 (s, 3H), 3.51 (t, J = 2.5 Hz, 1H). HRMS found for $M^+ + 1$, 376.1406, $C_{20}H_{17}N_5O_3$ requires 376.1404.

6-(1-(2,2-Difluoroethyl)-1H-pyrazol-4-yl)-2-(5,6-dimethoxypyridin-3-yl)-6,7-dihydro-5H-pyrrolo[3,4-b]pyridin-5-one (**12**). A 10 mL reaction vial was charged with **7** (50 mg, 0.148 mmol), cesium carbonate, (93 mg, 0.286 mmol), DMF (3 mL) and 2-bromo-1,1-difluoro-ethane (23 mg, 0.158 mmol). The vial was sealed and heated to 50 °C for 12 h. The reaction was diluted with water (55 mL) and extracted with EtOAc (30 mL). The organics were concentrated and purified by reverse phase chromatography (C18 column, 5-100% MeCN/H_2O containing 0.1% TFA) The product containing fractions were diluted with DCM, washed with saturated sodium bicarbonate and passed through a phase separator. The organics were concentrated to yield **12** (8.3 mg, 13%). ^{1}H NMR (400 MHz, DMSO-d_6) δ 8.56 (d, J = 2.0 Hz, 1H), 8.34 (d, J = 0.7 Hz, 1H), 8.27 - 8.12 (m, 2H), 7.99 (d, J = 2.0 Hz, 1H), 7.90 (d, J = 0.7 Hz, 1H), 6.52 - 6.26 (m, 1H), 4.99 (s, 2H), 4.69 (td, J = 15.1, 3.7 Hz, 2H), 3.94 (d, J = 14.3 Hz, 6H). HRMS found for M^+ + 1, 402.1375, $C_{19}H_{17}F_2N_5O_3$ requires 402.1372.

2-(4-(2-(5,6-Dimethoxypyridin-3-yl)-5-oxo-5,7-dihydro-6H-pyrrolo[3,4-b]pyridin-6-yl)-1H-pyrazol-1-yl)-2-methylpropanenitrile (**13**). Step 1: 4-nitro-1H-pyrazole (15.5 g, 137 mmol), 2-bromo-2-methyl-propanamide (25 g, 151 mmol), and K_2CO_3 (20.8 g, 151 mmol) were combined in DMF (200 mL) and heated to 50 °C for 24 h. The reaction was worked-up by pouring into EtOAc/1M NaOH (200 mL, 1:1). The organic layer was separated and washed with 1M NaOH, brine, dried over Na_2SO_4, filtered and concentrated to a white solid which was triturated with Et_2O and filtered to give **29** (9.7 g, 36%) as a white solid. The filtrate was concentrated and purified by flash column chromatography (330 g silica column, 0 to 100% EtOAc/hexane) to give additional product as a white solid (2.3 g). The total yield was 44% (12 g). ^{1}H NMR (300 MHz, DMSO-d_6) δ 8.95 (s, 1H), 8.29 (s, 1H), 7.32 (s, 1H), 7.21 (s, 1H), 1.75 (s, 6H). Mass spectrum (ESI) m/z 199.0 $[M + H]^+$.

Step 2: A Parr shaker bottle was charged with **29** (12.0 g, 60.6 mmol), MeOH (800 mL) and 10% Pd/C wet (6.4 g). The reaction was shaken under 40 psi H_2 on a Parr hydrogenator for 1 h. The reaction mixture was purged with N_2, filtered over Celite, and concentrated to provide **30** (10.1 g, 99%) as a coral colored solid. ^{1}H NMR (300 MHz, DMSO-d_6) δ 7.11 (s, 1H), 7.10 (s, 1H) 7.00 (s, 1H), 6.36 (s, 1H), 3.87 (s, 2H), 1.60 (s, 6H). Mass spectrum (ESI) *m/z* 169.0 $[M + H]^+$.

Step 3: Ethyl 6-chloro-2-(chloromethyl)pyridine-3-carboxylate (2.68 g, 11.5 mmol), **30** (2.12 g, 12.6 mmol) and DIPEA (4.0 mL, 22.9 mmol) were dissolved into anhydrous IPA (25 mL). The reaction was stirred 60 °C for 12 h. The reaction was cooled and the resulting precipitate was isolated via vacuum filtration and washed with IPA (2 x 25 mL) to provide **31** (1.67 g, 46%) as a yellow solid. ^{1}H NMR (300 MHz, DMSO-d_6) δ 8.22 (s, 1H), 8.18 (d, *J* = 8.1 Hz, 1H), 7.92 (s, 1H), 7.66 (d, *J* = 7.8 Hz, 1H), 7.21 (s, 1H), 6.85 (s, 1H), 4.92, (s, 2H), 1.73 (s, 6H). Mass spectrum (ESI) *m/z* 320.1 $[M + H]^+$.

Step 4: **31** (500 mg, 1.56 mmol) and 2,3-dimethoxy-5-(4,4,5,5-tetramethyl-1,3,2-dioxaborolan-2-yl)pyridine (456 mg, 1.72 mmol) were suspended in DME (30 mL) and aqueous Na_2CO_3 (2 M, 8 mmol) and sparged with N_2 for 10 min. To this solution was added $Pd(PPh_3)_4$ (181 mg, 0.156 mmol). The reaction was heated to 80 °C under N_2 for 4 h. After cooling to RT, the solvents were removed under reduced pressure and the resulting residue was suspended in water. The suspension was stirred vigorously for 10 min and the precipitate was then collected by vacuum filtration and washed water (2 x 30 mL). The filter cake was suspended in acetonitrile (30 mL). The suspension was heated to a boil, cooled to room temperature and the solid was isolated via filtration and dried further under high vacuum to provide **32** (440 mg, 66%). ^{1}H NMR (300 MHz, DMSO-d_6) δ 8.55 (s, 1H), 8.25-8.19 (m, 3H), 7.96 (d, *J* = 13.8 Hz, 2H), 7.25 (br s, 1H), 6.90 (br s, 1H), 4.98 (s, 2H), 3.93 (d, J = 10.8 Hz, 6H), 1.73 (s, 6H). Mass spectrum (ESI) m/z 423.2 $[M + H]^+$.

Step 5: 2-(4-(2-(5,6-dimethoxypyridin-3-yl)-5-oxo-5,7-dihydro-6*H*-pyrrolo[3,4-*b*]pyridin-6-yl)-1*H*-pyrazol-1-yl)-2-methylpropanamide **32** (400 mg, 0.946 mmol) and methyl *N*-(triethylammoniosulfonyl)carbamate (451 mg, 1.85 mmol) were combined in DCM (10 mL) and acetonitrile (10 mL) and stirred under nitrogen for 8 h at 60 °C in a sealed tube. The solvent was removed under reduced pressure; the resulting residue was dissolved in DCM (50 mL). The organics were washed with saturated aqueous Na_2CO_3, water, brine, dried over Na_2SO_4 and concentrated under reduced pressure. The residue was dissolved into DCM (10 mL) again and flushed through a plug of silica (20 g) with 1:1 DCM/EtOAc. After the organics were concentrated, the product was triturated with hexanes and isolated solid via vacuum filtration to provide **13** (311 mg, 81%). ^{1}H NMR (300 MHz, DMSO-d_6) δ 8.56 (d, 1H, J = 2.0 Hz), 8.43 (s, 1H), 8.2 (s, 1H), 8.19 (s, 1H), 8.07 (s, 1H), 7.98 (d, J = 2.0 Hz, 1H), 4.99 (s, 2H), 3.95 (s, 3H), 3.92 (s, 3H), 1.99 (s, 6H). HRMS found for $M^+ + 1$, 405.1669, $C_{21}H_{20}N_6O_3$ requires 405.1669.

3-(4-(2-(5,6-Dimethoxypyridin-3-yl)-5-oxo-5,7-dihydro-6H-pyrrolo[3,4-b]pyridin-6-yl)-1H-pyrazol-1-yl)propanenitrile (**14**). A 10 mL reaction vial was charged with **7** (50 mg, 0.148 mmol), cesium carbonate, (93 mg, 0.286 mmol), DMF (3 mL) and 3-bromopropanenitrile (21 mg, 0.158 mmol). The vial was sealed and heated to 50 °C for 12 h. The reaction was diluted with water and extracted with EtOAc. The organics were concentrated and purified by reverse phase chromatography (C18 column, 5-100% MeCN/H_2O containing 0.1%TFA). The product containing fractions were diluted with DCM, washed with saturated sodium bicarbonate and passed through a phase separator. The organics were concentrated to yield **14** (11.0 mg, 19%). ^{1}H NMR (300 MHz, DMSO-d_6) δ 8.56 (d, J = 2.0 Hz, 1H), 8.36 (s, 1H), 8.21 (t, J = 5.8 Hz, 2H), 7.99 (d, J = 2.0 Hz, 1H), 7.88 (s, 1H), 4.99 (s, 2H), 4.45 (t, J = 6.4 Hz, 2H), 3.96 (s, 3H), 3.92 (s, 3H), 3.09 (t, J = 6.4 Hz, 2H). HRMS found for M^+ + 1, 391.1520, $C_{20}H_{18}N_6O_3$ requires 391.1518.

(7S)-2-(5,6-Dimethoxy-3-pyridyl)-7-methyl-6-[1-(2,2,2-trifluoroethyl)pyrazol-4-yl]-7H-pyrrolo[3,4-b]pyridin-5-one (15) and (7R)-2-(5,6-dimethoxy-3-pyridyl)-7-methyl-6-[1-(2,2,2-trifluoroethyl)pyrazol-4-yl]-7H-pyrrolo[3,4-b]pyridin-5-one (**16**). Step 1: To a solution of 2-(5,6-dimethoxy-3-pyridyl)-6-[1-(2,2,2-trifluoroethyl)pyrazol-4-yl]-7H-pyrrolo[3,4-b]pyridin-5-one **10** (1.3 g, 3.07 mmol) and MeI (1.31 g, 9.21 mmol) in DMF (100 mL) at RT was added NaH (60 wt%, 123 mg, 3.07 mmol). After the reaction was stirred for 5 min another batch of NaH (60 wt%, 123 mg, 3.07 mmol) was added. The reaction was then stirred at rt for 1h. The reaction was cooled to 0 °C, quenched with saturated aqueous $NaHCO_3$ (3 mL), and then with water (150 mL). The solids were collected via vacuum filtration, washed with hot water and dried under high vacuum. After drying, the crude product was triturated with EtOH (10 mL x 5), to give 800 mg of racemic 2-(5,6-dimethoxy-3-pyridyl)-7-methyl-6-[1-(2,2,2-trifluoroethyl)pyrazol-4-yl]-7H-pyrrolo[3,4-b]pyridin-5-one which was resolved by chiral HPLC using a ChiralCel OD-H column, with 100% EtOH as the eluent to provide **15** (375 mg, 28%, 99.9% ee) as a white solid. ^{1}H NMR (300 MHz, DMSO-d_6) δ 8.58 (d, J = 1.9 Hz, 1H), 8.40 (s, 1H), 8.21 (q, J = 8.2 Hz, 2H), 8.00 (d, J = 1.9 Hz, 1H), 7.97 (s, 1H), 5.35 – 5.03 (m, 3H), 3.96 (s, 3H), 3.93 (s, 3H), 1.60 (d, J = 6.7 Hz, 3H). HRMS found for M^+ + 1, 434.1436, $C_{20}H_{18}F_3N_5O_3$ requires 434.1434. Compound **16** (370 mg, 27%, 99.8% ee) was also isolated as a white solid. ^{1}H NMR (300 MHz, DMSO-d_6) δ 8.58 (d, J = 1.9 Hz, 1H), 8.40 (s, 1H), 8.21 (q, J = 8.2 Hz, 2H), 8.00 (d, J = 1.9 Hz, 1H), 7.97 (s, 1H), 5.35 – 5.03 (m, 3H), 3.96 (s, 3H), 3.93 (s, 3H), 1.60 (d, J =

6.7 Hz, 3H). ^{19}F NMR (282 MHz, DMSO-d_6) δ -70.2 (t, J = 8.5 Hz). HRMS found for M^+ + 1, 434.1432, $C_{20}H_{18}F_3N_5O_3$ requires 434.1434.

2-(5,6-Dimethoxypyridin-3-yl)-7,7-dimethyl-6-(1-(2,2,2-trifluoroethyl)-1H-pyrazol-4-yl)-6,7-dihydro-5H-pyrrolo[3,4-b]pyridin-5-one (**17**). **10** (20 mg, 47.7 µmol) was dissolved in DMF (0.5 mL). To this solution was added MeI (17 mg, 0.119 mmol) followed by NaH (60 wt%, 6 mg, 0.143 mmol). The reaction was stirred at RT for 2 h and then quenched with saturated aqueous $NaHCO_3$ and extracted with DCM (75 mL). The organics were dried over Na_2SO_4, filtered, concentrated and purified by silica gel chromatography (4 g column, 0-20% MeOH in DCM) providing **17** (11 mg, 50%) as a white solid. ^1H NMR (300 MHz, $CDCl_3$) δ 8.45 (d, J = 1.9 Hz, 1H), 8.24 – 8.08 (m, 2H), 7.88-7.80 (m, 3H), 4.75 (q, J = 8.3 Hz, 2H), 4.08 (s, 6H), 1.72 (s, 6H). HRMS found for M^+ + 1, 434.1432, $C_{21}H_{20}F_3N_5O_3$ requires 434.1434.

ASSOCIATED CONTENT

The Supporting Information is available free of charge on the ACS Publications Website at DOI: xxxxxxx. Molecular Formula Strings (CSV), Descriptions of biochemical and cellular assays, Pharmacology, NMR spectra of **16**, Metabolite ID report for **6**, Crystallographic Information for **6**.

AUTHOR INFORMATION

Corresponding Authors

*Phone: 1-617-341-6838. Email jon_come@vrtx.com

*Phone: 1-617-341-6921. Email philip_collier@vrtx.com

*Phone: 1-617-341-6804. Email alex_aronov@vrtx.com

ABBREVIATIONS

CNS, central nervous system; DCM, dichloromethane; EAE, experimental autoimmune encephalomyelitis; fMLP, *N*-formyl-Met-Leu-Phe; GPCR, G-protein-coupled receptor; MCP-1, monocyte chemoattractant protein 1; MDCK, Madin Darby Canine Kidney; ND, no data; PgP, P-glycoprotein-1; ROS, reactive oxygen species.

PDB ID CODES: PDB ID Code for compound **6** is 6C1S. Authors will release the atomic coordinates and experimental data upon article publication. PDB IDs have been provided in figure legends.

All animal experiments were performed in compliance with institutional guidelines.

REFERENCES

1. Vanhaesebroeck, B.; Guillermet-Guibert, J.; Graupera, M.; Bilanges, B. The emerging mechanisms of isoform-specific PI3K signaling. *Nat. Rev. Mol. Cell Biol*. **2010**, *11*, 329−341.

2. Cantley, L. C. The phosphoinositide 3-kinase pathway. *Science* **2002**, *296*, 1655-1657.

3. Hawkins, P. T.; Anderson, K. E.; Davidson, K.; Stephens, L. R. Signalling through class I PI3Ks in mammalian cells. *Biochem. Soc. Trans.* **2006**, *34*, 647-662.

4. Fritsch, R.; de Krijger, I.; Fritsch, K.; George, R.; Reason, B.; Kumar, M. S.; Diefenbacher, M.; Stamp, G.; Downward, J. RAS and RHO families of GTPases directly regulate distinct phosphoinositide 3-kinase isoforms. *Cell* **2013**, *153*, 1050-1063.

5. Vadas, O.; Dbouk, H. A.; Shymanets, A.; Perisic, O.; Burke, J. E.; Abi Saab, W. F.; Khalil, B. D.; Harteneck, C.; Bresnick, A. R.; Nürnberg, B.; Backer, J. M.; Williams, R. L. Molecular determinants of PI3Kγ-mediated activation downstream of G-protein-coupled receptors (GPCRs). *Proc. Natl. Acad. Sci. USA* **2013**, *110*, 18862-18867.

6. Bi, L.; Okabe, I.; Bernard, D. J.; Wynshaw-Boris, A.; Nussbaum, R. L. Proliferative defect and embryonic lethality in mice homozygous for a deletion in the p110α subunit of phosphoinositide 3-kinase. *J. Biol. Chem*. **1999**, *274*, 10963-10968.

7. Bi, L.; Okabe, I.; Bernard, D. J.; Nussbaum, R. L. Early embryonic lethality in mice deficient in the p110β catalytic subunit of PI 3-kinase. *Mamm. Genome* **2002**, *13*, 169-172.

8. Guillermet-Guibert, J.; Smith, L. B.; Halet, G.; Whitehead, M. A.; Pearce, W.; Rebourcet, D.; León, K.; Crépieux, P.; Nock, G.; Strömstedt, M.; Enerback, M.; Chelala, C.; Graupera, M.; Carroll, J.; Cosulich, S.; Saunders, P. T. K.; Huhtaniemi, I.; Vanhaesebroeck, B. Novel role for p110β PI 3-Kinase in male fertility through regulation of androgen receptor activity in Sertoli cells. *PLOS Genet*. **2015**, *11*, e1005304.

9. Kong, D.; Yamori, T. Phosphatidylinositol 3-kinase inhibitors: promising drug candidates for cancer therapy. *Cancer Sci*. **2008**, *99*, 1734-1740.

10. Maira, S.-M.; Voliva, C.; Garcia-Echeverria, C. Class IA phosphatidylinositol 3-kinase: from their biological implication in human cancers to drug discovery. *Expert Opin. Ther. Targets* **2008**, *12*, 223-238.

11. Fruman, D. A.; Rommel, C. PI3K and cancer: lessons, challenges and opportunities. *Nat. Rev. Drug Disc*. **2014**, *13*, 140-156.

12. Kok, K.; Geering, B.; Vanhaesebroeck, B. Regulation of phosphoinositide 3-kinase expression in health and disease. *Trends Biochem. Sci*. **2009**, *34*, 115-127.

13. Laffargue, M.; Calvez, R.; Finan, P.; Trifilieff, A.; Barbier, M.; Altruda, F.; Hirsch, E.; Wymann, M. P. Phosphoinositide 3-kinase γ is an essential amplifier of mast cell function. *Immunity* **2002**, *16*, 441-451.

14. Ghigo, A.; Damilano, F.; Braccini, L.; Hirsch, E. PI3K inhibition in inflammation: toward tailored therapies for specific diseases. *BioEssays* **2010**, *32*, 185-196.

15. Siragusa, M.; Katare, R.; Meloni, M.; Damilano, F.; Hirsch, E.; Emanueli, C.; Madeddu, P. Involvement of phosphoinositide 3-kinase γ in angiogenesis and healing of experimental myocardial infarction in mice. *Circ. Res*. **2010**, *106*, 757−768.

16. Seropian, I. M.; Abbate, A.; Toldo, S.; Harrington, J.; Smithson, L.; Ockaili, R.; Mezzaroma, E.; Damilano, F.; Hirsch, E.; Van Tassell, B. W. Pharmacological inhibition of phosphoinositide 3-kinase gamma (PI3Kγ) promotes infarct resorption and prevents adverse cardiac remodeling after myocardial infarction in mice. *J. Cardiovasc. Pharmacol.* **2010**, *56*, 651-658.

17. Porcu, P.; Flinn, I.; Kahl, B. S.; Horwitz, S. M.; Oki, Y.; Byrd, J .C.; Sweeney, J.; Allen, K.; Faia, K.; Ni, M.; Stern, H. M.; Kelly, P.; O'Brien, S. Clinical activity of duvelisib (IPI-145), a phosphoinositide-3-kinase-δ,γ inhibitor, in patients previously treated with ibrutinib. *Blood* **2014**, *124*, 3335.

18. Hancox, U.; Cosulich, S.; Hanson, L.; Trigwell, C.; Lenaghan, C.; Ellston, R.; Dry, H.; Crafter, C.; Barlaam, B.; Fitzek, M.; Smith, P. D.; Ogilvie, D.; D'Cruz, C.; Castriotta, L.;

Wedge, S. R.; Ward, L.; Powell, S.; Lawson, M.; Davies, B. R.; Harrington, E. A.; Foster, E.; Cumberbatch, M.; Green, S.; Barry, S. T. Inhibition of PI3Kβ signaling with AZD8186 inhibits growth of PTEN-deficient breast and prostate tumors alone and in combination with docetaxel. *Mol. Cancer Ther*. **2015**, *14*, 48-58.

19. Okkenhaug, K.; Graupera, M.; Vanhaesebroeck, B. Targeting PI3K in cancer: impact on tumor cells, their protective stroma, angiogenesis, and immunotherapy. *Cancer Discov*. **2016**, *6*, 1090-1105.

20. Perry, V. H.; Holmes, C. Microglial priming in neurodegenerative disease. *Nat. Rev. Neurology* **2014**, *10*, 217-224.

21. Rommel, C.; Camps, M.; Ji, H. PI3Kδ and PI3Kγ: partners in crime in inflammation in rheumatoid arthritis and beyond? *Nat. Rev. Immun.* **2007**, *7*, 191-201.

22. Lull, M. E.; Block, M. L. Microglial activation and chronic neurodegeneration. *Neurotherapeutics*, **2010**, *7*, 354-365.

23. Camps, M.; Rückle, T.; Ji, H.; Ardissone, V.; Rintelen, F.; Shaw, J.; Ferrandi, C.; Chabert, C.; Gillieron, C.; Françon, B.; Martin, T.; Gretener, D.; Perrin, D.; Leroy, D.; Vitte, P.-A.; Hirsch, E.; Wymann, M. P.; Cirillo, R.; Schwarz, M. K.; Rommel, C. Blockade of PI3Kγ suppresses joint inflammation and damage in mouse models of rheumatoid arthritis. *Nat. Med.* **2005**, *11*, 936-943.

24. Mazaki, Y.; Nishimura, Y.; Sabe, H. GBF1 bears a novel phosphatidylinositol-phosphate binding module, BP3K, to link PI3Kγ activity with Arf1 activation involved in GPCR-

mediated neutrophil chemotaxis and superoxide production. *Mol. Biol. Cell.* **2012**, *23*, 2457-2467.

25. Li, D.; Park, D.; Abdul-Muneer, P. M.; Xu, B.; Wang, H.; Xing, B.; Wu, D.; Li, S. PI3Kγ Inhibition alleviates symptoms and increases axon number in experimental autoimmune encephalomyelitis mice. *Neuroscience*, **2013**, *253*, 89-99.

26. Pomel, V.; Klicic, J.; Covini, D.; Church, D. D.; Shaw, J. P.; Roulin, K.; Burgat-Charvillo, F.; Valognes, D.; Camps, M.; Chabert, C.; Gillieron, C.; Françon, B.; Perrin, D.; Leroy, D.; Gretener, D.; Nichols, A.; Vitte, P. A.; Carboni, S.; Rommel, C.; Schwarz, M. K.; Rückle, T. Furan-2-ylmethylene thiazolidinediones as novel, potent, and selective inhibitors of phosphoinositide 3-kinase γ. *J. Med. Chem*. **2006**, *55*, 3857−3871.

27. Cushing, T. D.; Metz, D. P.; Whittington, D. A.; McGee, L. R. PI3Kδ and PI3Kγ as targets for autoimmune and inflammatory diseases. *J. Med. Chem*. **2012**, *55*, 8559−8581.

28. Bell, K.; Sunose, M.; Ellard, K.; Cansfield, A.; Taylor, J.; Miller, W.; Ramsden, N.; Bergami, G.; Neubauer, G. SAR studies around a series of triazolopyridines as potent and selective PI3Kγ inhibitors. *Bioorg. Med. Chem. Lett*. **2012**, *22*, 5257−5263.

29. Oka, Y.; Yabuuchi, T.; Fujii, Y.; Ohtake, H.; Wakahara, S.; Matsumoto, K.; Endo, M.; Tamura, Y.; Sekiguchi, Y. Discovery and optimization of a series of 2-amino-thiazoloxazoles as potent phosphoinositide 3-kinase γ inhibitors. *Bioorg. Med. Chem. Lett*. **2012**, *22*, 7534−7538.

30. Oka, Y.; Yabuuchi, T.; Oi, T.; Kuroda, S.; Fujii, Y.; Ohtake, H.; Inoue, T.; Wakahara, S.; Kimura, K.; Fujita, K.; Endo, M.; Taguchi, K.; Sekiguchi, Y. Discovery of N-{5-[3-(3-

hydroxypiperidin-1-yl)-1,2,4-oxadiazol-5-yl]-4-methyl-1,3-thiazol-2-yl}acetamide (TASP0415914) as an orally potent phosphoinositide 3-kinase γ inhibitor for the treatment of inflammatory diseases. *Bioorg. Med. Chem.* **2013**, *21*, 7578−7583.

31. Leahy, J. W.; Buhr, C. A.; Johnson, H. W. B.; Gyu Kim, B.; Baik, T.; Cannoy, J.; Forsyth, T.; Jeong, J. W.; Lee, M. S.; Ma, S.; Noson, K.; Wang, L.; Williams, M.; Nuss, J. M.; Brooks, E.; Foster, P.; Goon, L.; Heald, N.; Holst, C.; Jaeger, C.; Lam, S.; Lougheed, J.; Nguyen, L.; Plonowski, A.; Song, J.; Stout, T.; Wu, X.; Yakes, M. F.; Yu, P.; Zhang, W.; Lamb, P.; Raeber, O. Dicovery of a novel series of potent and orally bioavailable phosphoinositide 3-kinase γ inhibitors. *J. Med. Chem*. **2012**, *55*, 5467−5482.

32. Sunose, M.; Bell, K.; Ellard, K.; Bergamini, G.; Neubauer, G.; Werner, T.; Ramsden, N. Discovery of 5-(2-amino-[1,2,4]triazolo[1,5-a]pyridin-7-yl)-N-(tert-butyl)pyridine-3-sulfonamide (CZC24758), as a potent, orally bioavailable and selective inhibitor of PI3K for the treatment of inflammatory disease. *Bioorg. Med. Chem. Lett.* **2012**, *22*, 4613-4618.

33. Evans, C. A.; Liu, T.; Lescarbeau, A.; Nair, S. J.; Grenier, L.; Pradeilles, J. A.; Glenadel, Q.; Tibbitts, T.; Rowley, A. M.; DiNitto, J. P.; Brophy, E. E.; O'Hearn, E. L.; Ali, J. A.; Winkler, D. G.; Goldstein, S. I.; O'Hearn, P.; Martin, C. M.; Hoyt, J. G.; Soglia, J. R.; Cheung, C.; Pink, M. M.; Proctor, J. L.; Palombella, V. J.; Tremblay, M. R.; Castro, A. C. Discovery of a selective phosphoinositide-3-kinase (PI3K)-γ inhibitor (IPI-549) as an immuno-oncology clinical candidate. *ACS Med. Chem. Lett.* **2016**, *7*, 862-867.

34. Aronov, A. M.; Murcko, M. A. Toward a pharmacophore for kinase frequent hitters. *J. Med. Chem.* **2004**, *47*, 5616-5619.

35. Trippier, P. C. Selecting good 'drug-like' properties to optimize small molecule blood-brain barrier penetration. *Curr. Med. Chem.* **2016**, *23*, 1392-1407.

36. Collier, P. N.; Martinez-Botella, G.; Cornebise, M.; Cottrell, K. M.; Doran, J. D.; Griffith, J. P.; Mahajan, S.; Maltais, F.; Moody, C. S.; Huck, E. P.; Wang, T.; Aronov, A. M. Structural basis for isoform selectivity in a class of benzothiazole inhibitors of phosphoinositide 3-kinase γ. *J. Med. Chem*. **2015**, *58*, 517-521.

37. Collier, P. N.; Messersmith, D.; Le Tiran, A.; Bandarage, U. K.; Boucher, C.; Come, J.; Cottrell, K. M.; Damagnez, V.; Doran, J. D.; Griffith, J. P.; Khare-Pandit, S.; Krueger, E. B.; Ledeboer, M. W.; Ledford, B.; Liao, Y.; Mahajan, S.; Moody, C. S.; Roday, S.; Wang, T.; Xu, J.; Aronov, A. M. Discovery of highly isoform selective thiazolopiperidine inhibitors of phosphoinositide 3-kinase γ. *J. Med. Chem*. **2015**, *58*, 5684-5688.

38. Pierce, A.; Sandretto, K. L.; Bemis, G. W. Kinase inhibitors and the case for CH•••O bonds in protein-ligand binding. *PROTEINS: Struct., Funct., Gen.* **2002**, *49*, 567-576.

39. Pierce, A. C.; ter Haar, E.; Binch, H. M.; Kay, D. P.; Patel, S. R.; Li, P. CH•••O and CH•••N hydrogen bonds in ligand design: a novel quinazolin-4-ylthiazol-2-ylamine protein kinase inhibitor. *J. Med. Chem*. **2005**, *48*, 1278-1281.

Table of Contents graphic